



Seakeeping Committee

Final Report and Recommendations to the 27th ITTC

1. GENERAL

1.1. Membership and meetings

The Committee appointed by the 26th ITTC consisted of the following members :

- Yonghwan Kim (Chairman), Seoul National University, Korea
- Dan Hayden (Secretary), Naval Surface Warfare Center, West Bethesda, USA
- Dariusz Fathi, Norwegian Marine Technology Research Institute (MARINTEK), Trondheim, Norway
- Greg Hermanski, Institute for Ocean Technology, St. John's, Canada
- Dominic Hudson, University of Southampton, United Kingdom
- Pepijn de Jong, Delft University of Technology, The Netherlands
- Katsuji Tanizawa, National Maritime Research Institute, Tokyo, Japan
- Giles Thomas, Australian Maritime College, University of Tasmania, Tasmania, Australia
- Wu Chengshen, China Ship Scientific Research Center, Wuxi, China (Replaced Dr. Quanming Miao in 2012)

Four committee meetings were held at:

- University of Southampton, Southampton, United Kingdom, January 2012
- National Maritime Research Institute, Tokyo, November 2012.
- David Taylor Model Basin, West Bethesda, USA, July 2013
- Delft University of Technology, Delft, Netherlands, February 2014

In addition, a joint ISSC/ITTC workshop on uncertainty modelling for ships and offshore structures was held in Rostock, Germany in September 2012.

1.2. Terms of Reference Given by the 26th ITTC

The list of tasks recommended by the 26th ITTC was as follows:

1. Update the state-of-the-art for predicting the behaviour of ships in waves emphasising developments since the 2011 ITTC Conference. The committee report should include sections on:
 - a. the potential impact of new technological developments on the ITTC
 - b. new experiment techniques and extrapolation methods,
 - c. new benchmark data



- d. the practical applications of computational methods to seakeeping predictions and scaling.
 - e. the need for R&D for improving methods of model experiments, numerical modelling and full-scale measurements.
2. Review ITTC Recommended Procedures relevant to seakeeping and
 - a. Identify any requirements for changes in the light of current practice, and, if approved by the Advisory Council, update them.
 - b. Identify the need for new procedures and outline the purpose and content of these.
 - c. Introduce a definition of slamming.
 3. Liaise with ISSC, the Ocean Engineering Committee, The Stability in Waves Committee and the Specialist Committee on Performance of Ships in Service.
 4. Update existing ITTC Recommended Procedure 7.5-02-07-02.5, Verification and Validation of Linear and Weakly Non-Linear Seakeeping Codes, to reflect the outcomes of the Verification and Validation workshop held in 2010.
 5. Investigate methodology for Verification and Validation of fully non-linear seakeeping viscous flow codes.
 6. Develop a guideline for the verification and outline further developments required for validation of hydroelastic seakeeping codes.
 7. Jointly organize and participate in the joint ISSC/ITTC workshop on uncertainty in measurement and prediction of wave loads and responses.
 8. Establish a numerical and experimental process for estimating f_w , in the EEDI calculation. Liaise with the Specialist Committee on Performance of Ships in Service.
 9. Develop a unified method for sloshing experiments drawing on the methods developed by the classification societies. Identify benchmark data for sloshing in LNG carriers.
 10. Review and update the Procedure 7.5-02-05-04, Seakeeping Tests for High Speed Marine Vehicles.

2. REVIEW OF STATE-OF-THE-ART

2.1. New Experimental Facilities

2.1.1. Actual Sea Model Basin, National Maritime Research Institute

The Actual Sea Model Basin (Figure 1) is a very advanced indoor facility for the simulation of the actual sea environment, including wind and waves, constructed at the National Maritime Research Institute and completed at the end of August 2010. The length, width and depth of the basin are 80m, 40m and 4.5m, respectively. A total of 382 segmented flap-type absorbing wave makers are installed on all peripheries of the basin. By numerical control of individual segments, realistic wave field of the actual seas can be reproduced in the basin. For model tests, a three degree of freedom towing carriage is available. The main carriage, which has a rail span of 41m, travels up to 3.5m/s, and the sub-carriage installed below the main-carriage runs up to 3.0m/s and is equipped with a turntable. In addition to multi-functional towing capability, auto-tracking function is available for free running tests in waves. For wind generation, removable blow-



ers are available and a fluctuating wind up to 10m/s can be generated. The basin has a central control system of the wave makers, towing carriages and the wind generators. All functions of this basin are controlled synchronously. As a result, a high level of accuracy and reproducibility are achieved.

The Actual Sea Model Basin is a rectangular tank with rounded corners. Dimensions of the basin and its trimming tank are given in Table 1 and Table 2. For the installation about 2 meters of space is required at the backside of the flap. As a result, size of the water surface is about 76m x 36m. The four corners radius of curvature is 7.70m.

The Actual Sea Model Basin has 382 flap type absorbing wavemakers along the entire periphery except in front of the trim tank. The flap boards of the unit are connected to neighbors by watertight fan-like connection plates to avoid discontinuity. Each unit is numerically controlled both for generation and absorption and the entire water surface can be used for uniform wave field even in the case of short crested irregular wave generation.

The Actual Sea Model Basin has a X-Y- ϕ towing carriage. Main carriage travels the longitudinal X direction, sub-carriage installed below the main carriage travels the transverse Y direction and the turntable installed on the sub-carriage rotate ϕ direction around vertical axis.



Figure 1. New actual sea model basin at NMRI

Table 1. Dimension of Actual Sea Model Basin

Length	Between Wall	80.0 m
	Water Surface	76.2 m
Width	Between Wall	40.0 m
	Water Surface	36.0 m
Depth	---	4.95 m
Water Depth	Standard	4.50 m

Table 2. Dimension of Trimming Tank.

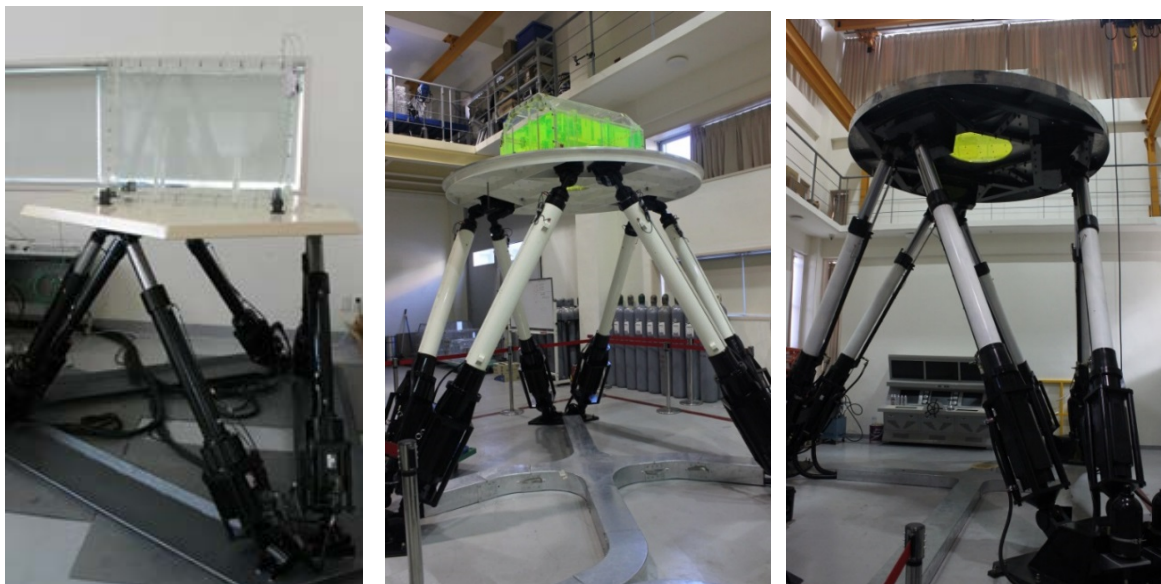
Length	6.0 m
Width	1.2 m
Depth	0.95 m
Water Depth	0.65 m

2.1.2. Seoul National University Sloshing Facility

Recently Seoul National University (SNU) installed three hexapod motion platforms with different payloads: 1.5 tonne, 5 tonne and 14 tonne (Figure 2). Each platform has six linear motors of different capacities, and all platforms are capable of simulating the 6-DOF motions of ships in a seaway. The small and midsize platforms of 1.5 tonne and 5 tonne capacity were installed in 2009, but the large platform of 14 tonne capacity including mount base was installed in 2012 and upgraded twice in 2013. The large platform height is 4.0m at rest condition, 4.9m in stand-by condition, and about 5.7m in maximum heave motion. This platform consumes 140kW in normal/average excitation condition and 270kW in peak excitation. The detailed kinematic performance is summarized in the Table 3.

The small platform of 1.5 tonne payload is suitable for the 3D model tests of about 1/70 scale, and the midsize platform of 5 tonne payload can be used for the 3D model tests of 1/60~1/40 scale. The large platform of 14 tonne payload can be used for the 3D model of 1/40~1/20 scale, but the experiment becomes more expensive as the size of model increases. Figure 3 shows the relative scale of the three motion platforms.

The facility at SNU is the world’s largest sloshing experimental facility, with 500 dynamic, high quality pressure sensors, associated DAQ system and about 160TB storage for data acquisition and storage. 2D and 3D PIV systems are available in this facility. The heavy-gas test using SF6 and N2 is also carried out in this test facility.



(a) 1.5 tonne platform

(b) 5 tonne platform

(c) 14 tonne platform

Figure 2. Three hexapod motion platforms in SNU

Table 3. Performance of 14 tonne Hexapod Platform

	Displacement	Speed		Acceleration
		@1500 rpm	@2000 rpm	
Surge	±144 cm	155 cm/s	200 cm/s	> 0.9G
Sway	±138 cm	138 cm/s	180 cm/s	> 0.9G
Heave	±84 cm	84 cm/s	110 cm/s	> 0.9G
Roll	±33°	34°/s	45 °/s	> 250°/s ²
Pitch	±33°	37°/s	49 °/s	> 250°/s ²
Yaw	±33°	56°/s	74 °/s	> 250°/s ²

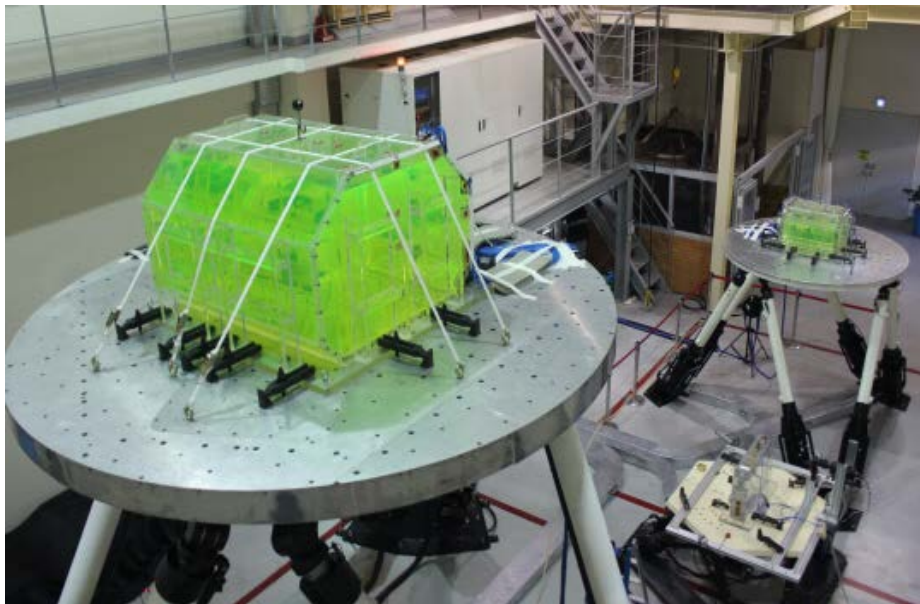


Figure 3. Scaled model tanks on the large and midsize platforms and a 2D tank on the small platform



Figure 4. New Wavemaking Facility in Maneuvering and Seakeeping Basin (MASK), CDNSWC

2.1.3. New Wavemaker – MASK Basin, Naval Surface Warfare Center

A wavemaker replacement for the Maneuvering and Seakeeping Basin, of Carderock Division, Naval Surface Warfare Center was publicly completed in December 2013 (Figure 4). The wavemaker machine consists of 216 paddles at a 0.658 m spacing from centreline to centreline. There are 108 paddles along the long wall of the tank, 60 paddles in the curve, and 48 paddles along the short wall. The paddles have a hinge depth of 2.5 meters. The wavemaker is of a dry-back design with gusset material connecting each paddle. The paddles integrate a force feedback design where forces are measured at the lower hydrostatic assist location and at the upper motion control attachment. The components of the wavemaker are illustrated in Figure 5. The new wavemaker is capable of regular and irregular seas, multi-component long and short crested seaways, and other superposition events as required. No changes in the beaches along the opposite sides of the basin were required.

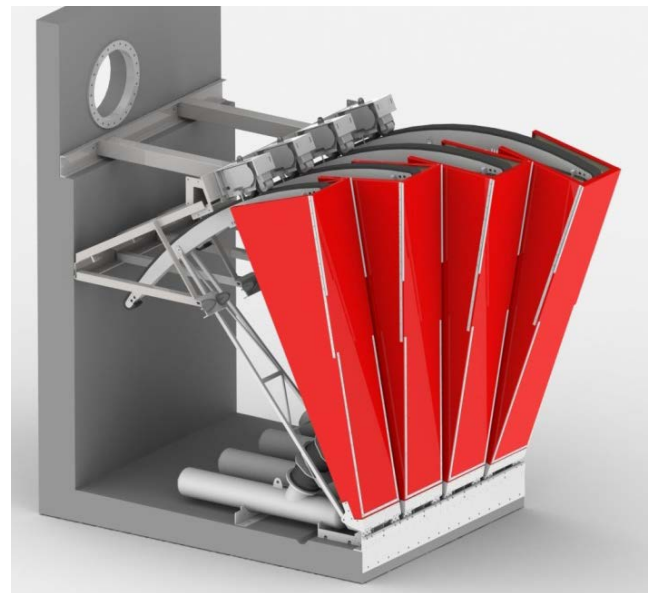


Figure 5. Rendering of 4 MASK Wavemaker Paddles Showing Components

2.1.4. New Wavemaker – Depressurized Wave Basin, MARIN

A wavemaker replacement for the depressurized basin of the MARIN facility was publicly completed in March 2012. In tandem with the wavemaker upgrade, several new sub carriages were built due to the improvement of



having wavemakers installed in the depressurized wave basin as shown in Figure 6. The wavemaker installation includes 24 dry-back paddles with a 2.5m hinge depth and a 0.6m width along the short wall; and 200 dry-back paddles with a 1.8m hinge depth and 0.6m width along the long edge. The junction of the short and long walls is shown in Figure 7. Both banks of paddles were similar in design concept to the components shown in Figure 5 for the MASK basin as both designs were provided by the same company. Deployable beaches were installed as required on opposite walls since wavemakers had not previously been installed. The wavemakers had to be designed and built to satisfy the unique challenges of a depressurized facility.

The wavemaking capability in a depressurized basin will allow for the investigation of air-water phenomena not previously possible. These areas of investigation could include damaged stability, cavitation, designed air cavities, and air cavities during slamming and wave impacts.



Figure 6. New wavemakers and sub carriages at MARIN depressurized basin



Figure 7. New wavemakers at junction of short and long walls of depressurized basin

2.1.5. New Towing Tank, University of Southampton

A new towing tank is under construction at the University of Southampton, UK, due for completion in September 2014. The new facility is 138m long with a breadth of 6m and a depth of 3.5m. The tank is equipped with a cable-driven carriage having a maximum speed of 12 m/s. The Wolfson Unit for Marine Technology and Industrial Aerodynamics, part of the University of Southampton, and the University's Ship Science degree programme will be the primary users of the facility. The tank is designed to allow all types of hydromechanic experiments for the shipping, offshore and yacht and small craft industries. The towing tank will be used for a mix of activities including education, research and consultancy. Seakeeping experiments will be performed with hinged-flap wavemakers, which are capable of generating regular and irregular waves as well as transient breaking and focused waves. The maximum wave height for regular waves is 0.5m and waves with a period between 0.8s and 3.5s can be generated. Both standard and user-defined sea-states can be used. The tank is also to be equipped with a motion-tracking camera system and PIV for fluid flow diagnostics. A small coastal wave basin (5m x 5m), narrow flume with wavemakers and three wind



tunnels are also included in the purpose-built fluid dynamics laboratory building.

2.2. Development in Experimental, Analytical, and Numerical Techniques

2.2.1. Experimental Techniques

This section contains reviews of work concerning developments in experimental techniques, which include model scale and full scale experiments.

2.2.1.1. Model Scale Experiment

Added resistance / speed loss in waves

The prediction of added resistance or speed loss of a ship in waves is essential to evaluate the ship performance in a seaway. In the past several decades, experimental techniques on added resistance in waves have been well developed, especially for ships in long and intermediate-length waves. However, experiments for added resistance in short waves are still a challenge to many researchers.

Some of the modern ships are very large, for example, a VLCC (Very Large Crude-oil Carrier) will exceed 320m in length. That means when the VLCC is travelling in normal sea states, most of the waves encountered can be considered as short waves. So the prediction of added resistance for ships in short waves is an important topic.

One of the major challenges is the generation of short waves with high quality in wave basin. Waves with high steepness are unstable (called the Benjamin-Feir instability effect), and short waves with low steepness are subject to more spatial variation than long waves due to the variation in their transversal amplitude across the basin. The generation of short waves

is also restricted by the characteristics of the wave generator.

Guo and Steen (2011) carried out an experimental study on the added resistance of KVLCC2 in short waves. The shortest wave length for model test is about $0.18L_{pp}$. A unique feature of this experiment is that the ship model is divided into three segments: fore-segment, aft-segment, and parallel mid-body. An aluminium frame is used to keep the three segments together. The fore- and aft- segments are connected to the frame through springs and force transducers. The springs only absorb vertical forces, whereas the force transducers measure the longitudinal forces. The added resistance distribution with respect to the hull segments can be explored through this method. Before the experiment, a detailed wave calibration was carefully performed. A new data processing method was proposed to eliminate the effect of low-frequency noise in the measured force to achieve more accurate results.

The experimental results show that the added resistance is concentrated at the fore segment and that it is small at the aft segment. In the mid segment, the increase of frictional resistance due to short waves is very small (Figure 8). The non-dimensional added resistance coefficient measured by the experiment is fairly independent of wave amplitude, which confirms that the added resistance for short waves is roughly proportional to the square of the wave amplitude.

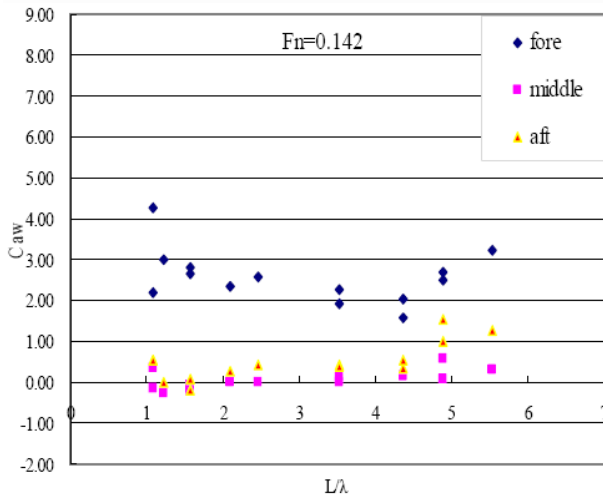


Figure 8. Added resistance with respect to hull segments

The effect of oblique waves on ocean-going vessel behaviour in realistic sea states was studied by Chuang and Steen (2013). Seakeeping model tests were carried out with a free running model in oblique waves in the ocean basin laboratory. Calm water resistance, azimuth propulsion system, ship machinery, seakeeping, steering and automatic control were all included in the model tests. In order to compensate for the relatively higher frictional resistance of the model, a tow rope force was applied by an air fan mounted on the model. Due to the limitation of the experimental environment, converged speed in waves could not be achieved in all runs. A correction method was also proposed to find converged speed from non-converged model tests.

The experimental results show that in oblique waves, the speed loss increase with the added wave resistance (Figure 9). When wave length approaches ship length, the speed loss reaches its peak value. For a fixed heading angle, speed loss is increasing roughly linearly with increasing wave elevation for tests with constant propulsive power. When the power is kept constant in head sea and bow sea conditions, the higher the initial calm water speed, the less will the speed drop in waves.

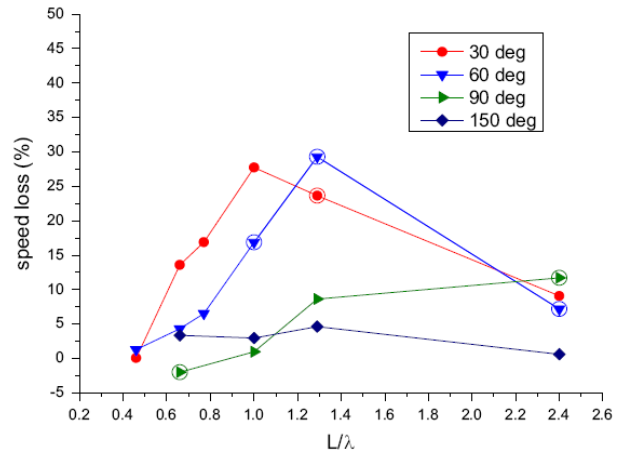


Figure 9. Experimental speed loss in waves

Tanizawa, K. (2012) and Kitagawa, Y (2014) introduced an experimental methodology for free running test to measure the nominal speed loss in waves. They developed two devices. One is a marine diesel engine simulator, MDES. Based on the mathematical model of a marine diesel engine, MDES controls the propeller rotational speed of model ships by real time simulation of engine response to the propeller loading oscillation. With MDES, engine characteristics could be considered in the model test. The other is an auxiliary thruster system, ATS. This is a duct fan working in the air to add thrust to the model ship in order to correct for differences in skin friction. With ATS, the propeller loading condition of model ship could be adjusted to that of the full-scale ship at the same Froude number. They conducted a free running model experiment in waves using the MDES and ATS and measured not only ship motion responses but also the realistic dynamic responses of a ship propulsion system in waves such as propeller load and rotating speed oscillation, fuel supply rate and nominal speed loss in waves.

Influence of abnormal waves

Abnormal wave encounters can result in significant damage to or loss of a vessel. Sig-

nificant attention should be paid to identifying the risks to a vessel when encountering abnormal waves.

Clauss and Klein (2011) investigated the generation, propagation, kinematics and dynamics of extreme waves in a seakeeping basin. The measurements were conducted in the seakeeping basin of the Ocean Engineering Division, Technical University of Berlin. The spatial development of the extreme wave was measured in a range from 30.9m ahead of, to 21.0m behind the target position for a total of 520 registrations. The towing carriage was equipped with 13 wave gauges installed at an interval of 0.2m and the seakeeping basin was subdivided into 20 measurement sections. Figure 10 shows the experimental set-up schematically, with a side view on the set-up (top) describing the measurement orders as well as a top view on the arrangement of the wave gauges installed on the towing carriage (bottom).

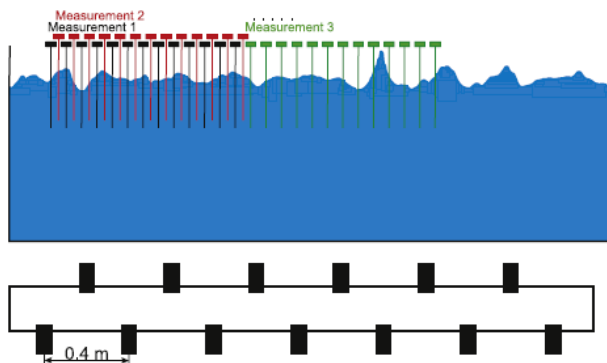


Figure 10. Schematic sketch of the extreme wave experimental set-up

The impact of the extreme wave on a ship was also investigated, in particular the vertical bending moment. A Ro/Ro vessel in the extreme wave in head seas was studied (Figure 11). The wooden model was subdivided into three segments intersected at $L_{pp}/2$ and $3/4L_{pp}$ (measured from the A.P.). The segments were connected by three force transducers at each

cut. The force transducers registered the longitudinal forces during the model tests. The vertical wave bending moment superimposed by the counteracting vertical bending moment caused by the longitudinal forces can be determined based from the measured forces. Figure 12 shows an example of experimental vertical bending moment (VBM) time traces.



Figure 11. Model test of a Ro/Ro vessel in an extreme wave

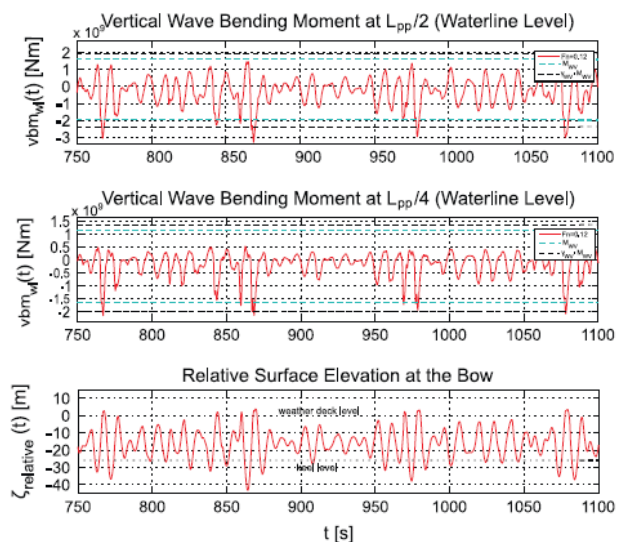


Figure 12. Experimental results of VBM for vessel in abnormal sea states

The analysis of the registrations reveal extreme waves occurring at three different positions in the seakeeping basin, emerging from a

wave group, which propagates almost constantly along the wave tank. The analysis of the total energy propagation shows that the wave crest velocity of the three waves in the wave group, i.e. the celerity is almost twice the velocity of the mean energy (group velocity). The investigations on wave-structure interaction between such an extraordinarily high wave and a segmented wooden Ro/Ro ship model reveal that the impact is severe and results in high global loads.

Bennett et al. (2012) carried out an experimental investigation of global symmetric wave-induced loads, as well as motions, experienced by a naval ship (a frigate) in abnormal waves. Experiments were conducted using a segmented flexible backbone model in regular and irregular (random and abnormal) sea states at forward speed. Abnormal sea states were generated using a previously developed optimisation technique. Measurements were made of symmetric motions and the vertical bending moment at various locations along the ship. The influence of slamming on severity of abnormal wave encounters was discussed.

Water on deck and slamming

Green-water events are well recognised as dangerous circumstances for marine vehicles in general. They are characterized by compact masses of liquid shipped onto the vessel deck due to the ship interactions with sufficiently severe sea states and their consequences can affect stability, structural integrity, operations on board and safety, depending on the vessel type and operational conditions. Slamming is another phenomenon of concern for ships and may occur in connection with water-shipping events, complicating the wave-ship interaction scenario. It is associated typically to small spatial and temporal scales, with location and features depending on the vessel geometry and operational conditions.

A synchronic 3-D experimental investigation was conducted by Greco et al. (2012) for wave-ship interactions involving the water-on-deck and slamming phenomena. The experiments examined a patrol ship at rest and with forward speed that was free to oscillate in heave and pitch in regular and irregular waves (Figure 13). In the study, the head-sea regular wave conditions were examined in terms of (1) RAOs and relative motions, (2) occurrence, features and loads of water-on-deck, bottom-slamming and flare-slamming events and (3) added resistance in waves. A systematic and comprehensive analysis of the phenomena was made available in terms of the Fr , incoming wavelength-to-ship length ratio and wave steepness. The main parameters that affect the global and local quantities were identified and possible danger in terms of water-on-deck severity and structural consequences were determined. Different slamming behaviors were identified, depending on the spatial location of the impact on the vessel: single-peak, church-roof and double-peak behaviors. A bottom-slamming criterion was assessed.



Figure 13. Model test of water on deck and slamming

Thomas et al. (2011), Lavroff et al. (2013) investigated slam events experienced by high-speed catamarans in irregular waves through experiments using a hydroelastic segmented

model (Figure 14). It was tested in irregular head seas at two speeds relating to Fr of 0.32 and 0.60. Nearly 300 slams were identified in the test data and analyzed with respect to kinematic parameters. Slams were found to have a large range of magnitudes; however, the majority of events were of relatively low severity. Differences in slam characteristics were found for two model speeds tested.



Figure 14. Slamming on the centre bow of the catamaran model

Sloshing

Wave-impact in sloshing flows is an important issue for the safety of the LNG carriers. Ji et al. (2012) carried out experiments on non-resonant sloshing in a rectangular tank with large amplitude lateral oscillation. A sequence of experiments was performed to investigate large amplitude sloshing flows at off-resonant condition far from the system natural frequency. Through PIV measurement, it showed that the flow physics on nonlinear off-resonant sloshing problem can be characterized into a combination of three peculiar sloshing motions: standing wave motions, run-up phenomenon and gradually propagating bore motion from one sidewall to the opposite wall.

Bardazzi et al. (2012) carried out an experimental study on the kinematic and dynamic features of a wave impacting a rigid vertical

wall of a 2D sloshing tank in the shallow water condition. The strain distribution along a vertical aluminium plate inserted in a rigid vertical wall of a sloshing tank was measured to characterize the dynamic features of the local loads. To assess the effect of the hydroelasticity, the same phenomenon was reproduced on the opposite fully rigid wall of the tank. The experimental results show that although the overall kinematical evolution of the phenomenon is quite well reproduced, strong differences were observed in the dynamical features between elastic and rigid case.

Loads due to sloshing in LNG tanks not only act on tank walls as inner loads, but also affect the global wave loads by coupling with general motions of the carrier. Wang et al. (2012) investigated sloshing and its effects on global responses of a large LNG carrier. In their experiments, the interactions of sloshing motions and the global wave loads were studied by seakeeping model tests of a self-propelled LNG ship with a liquid tank (Figure 15). The results show that the existence of liquid in tank will affect the vertical natural frequencies of the hull girder and natural rolling period of the ship. The motion period of liquid in the tank depends on the inner shape of the tank and the filling level, and on the wave heading and ship speed. The general effects of sloshing on global wave loads are not very remarkable, though the wave direction and ship speed are the sensitive parameters of the LNG carrier relative to sloshing.



Figure 15. Model test of LNG carrier with liquid tank

Other issues

Tiao (2011) carried out an experimental investigation of nonlinearities of ship responses in head waves. The experimental program consisted of tests in both regular and irregular head waves, and the measured quantities included wave elevation, vertical motions, and hull pressures. By contrasting these results to the quasi-linear behaviours of heave motion, the nonlinear behaviours of pressure were highlighted and presented. Three nonlinear assessments, the probability density function, and the variance spectra were provided.

Hashimoto et al. (2011) carried out the broaching prediction of a wave-piercing tumblehome vessel with twin screws and twin rudders (Figure 16). In their study, a series of captive model tests were conducted to measure the resistance, the manoeuvring forces, the wave-exciting forces, the heel-induced hydrodynamic forces, and the roll restoring variation for the vessel.

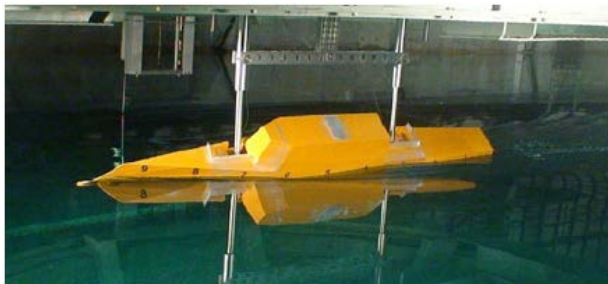


Figure 16. Captive model test for broaching

2.2.1.2. Full Scale Experiment

Full-scale measurements are an extremely effective mechanism for investigating seakeeping behaviour, although they are complex and expensive to conduct.

Jacobi et al. (2013) investigated the slamming behaviour of large high-speed catamarans through full-scale measurements. The US Navy conducted the trials in the North Sea and North

Atlantic region on a 98m wave piercer catamaran. For varying wave headings, vessel speeds and sea states the data records were interrogated to identify slam events. An automatic slam identification algorithm was developed. This has allowed the slam occurrence rates to be found for a range of conditions and the influence of vessel speed, wave environment and heading to be determined. The slam events were further characterized by assessing the relative vertical velocity at impact between the vessel and the wave.

Koning and Kapsenberg carried out a measurement campaign on board a 9,300 TEU container vessel. The measurements comprised ship performance parameters, cross section loads on two locations, local stresses in the bow area and accelerations on five longitudinal locations on deck. The wave environment was monitored by wave radar analyzing the back scatter from the waves and by two height level radars on the bow. Figures 17 and 18 show sample full scale time traces.

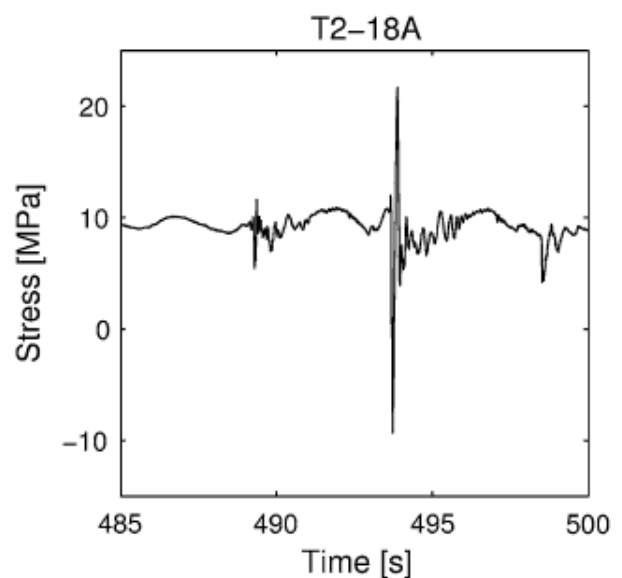


Figure 17. Sample full scale raw strain gauge data showing slam events

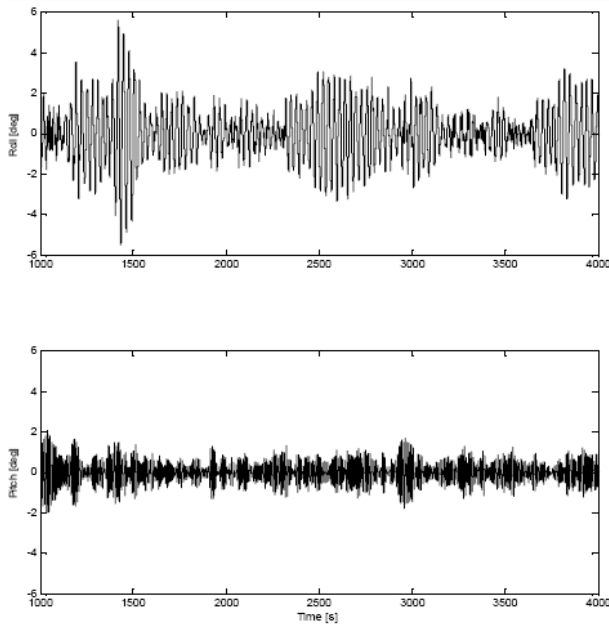


Figure 18. Full scale rigid body motions: roll and pitch

2.2.2. Numerical Methods

Frequency Domain Methods for Motions and Loads

Due to the advances that have been made in the development and validation of time domain methods in recent years there is a visible shift in the literature from frequency based methods towards time domain methods. This shift in focus has reached the point where in application time domain methods are now superseding frequency domain methods to a large extent.

Nonetheless, in the early design stage frequency domain methods prove more efficient in providing quick solutions, allowing for the evaluation of a large amount of design alternatives at a lower level of detail and complexity. Also for the analysis of typical zero or slow speed applications such as moored floating structures in waves and current and in particular for multi-body problems as side-by-side moored systems, the frequency domain method

still proves to be a reliable and efficient solution.

There has been recent work done on improving the numerical properties of frequency domain methods. Du et al. (2012) studied the occurrence of irregular frequencies for zero and for forward speed problems. They found that for most applications irregular frequencies occur outside the range of practical interest for rigid body motions. However difficulties can occur in the analysis of large offshore structures and in hydro-elastic problems of flexible bodies. They implemented a lid method to suppress the occurrence of irregular frequencies at zero speed. Their work also shows that while irregular frequencies may not occur with forward speed, the disturbances can be caused by inaccurate treatment of the waterline integral terms and the solution method as the forward speed tends to smaller values.

Nan and Vassalos (2012) discuss the treatment of the m-terms in a forward speed frequency domain method. M-terms are second order derivatives of the steady flow potential that appear in the body boundary condition. In their study they evaluated the m-terms explicitly with a numerical scheme in a frequency domain Rankine panel method. They showed agreement between the predictions from their method and model experiments.

As an example of the application of frequency domain methods in design applications, Tello et al. (2011) presented a study of the seakeeping performance of a set of fishing vessels applying a linear three-dimensional frequency domain method. Maximo et al. (2012) used a linear frequency domain panel code to evaluate the seakeeping performance of a high speed trimarans vessel in a parametric design tool for rapid evaluation of various design solutions.



As an illustration of the usage of frequency domain methods for zero speed applications, Wang and Xie (2012) combined a linear frequency domain method to compute the first order wave induced motions with mean and low frequency drift motions estimated from pre-computed drift design curves for a floating offshore unit. For the pre-computed drift motion design curves use was made of a nonlinear coupled time domain analysis.

Zhao et al. (2011) investigated the interactions between the motions and inner-tank sloshing of a FNLG using a frequency domain method. They included the interior wetted surface of the tanks as conventional outer wetted surface and evaluated the effect of sloshing on the global response by comparing responses with and without the effect of sloshing.

Time Domain Methods for Motions and Loads

Time domain methods have gained increasing interest and many alternative methods have been developed over the last few decades. At this moment, time domain methods seem to be displacing the more traditional frequency domain methods for many practical applications. The advantage of time domain methods lies in the more intuitive extension towards nonlinear motions and loads and the relative ease of incorporating external forces, such as propulsion and control forces or coupling with flexible structural modes and sloshing problems. This usually comes at the cost of an increased computational demand compared to frequency domain methods. Especially for the more nonlinear approaches dealing with the geometry, for instance generating a panelization on the time dependent wetted surface can be a significant task.

There are many alternative time domain solutions being developed and used for practical

applications. These range from two dimensional linear or nonlinear strip theory to three dimensional transient Green Function Methods (GFM) and Rankine Panel Methods (RPM). Emerging alternative potential flow based techniques are Higher Order Boundary Element Methods (HOBEM) and nonlinear potential flow Finite Element Methods (FEM). In some cases hybrid methods are being proposed.

(i) 2D time domain techniques

Two dimensional time domain methods are relatively efficient and less complex in development compared to three dimensional time domain approaches. Often they are based on frequency domain methods that are extended to the time domain by using retardation functions. Time domain based solutions exist and are often applied for high speed planing problems.

Chuang and Steen (2013), for example, computed the speed loss of a vessel in oblique waves by combining linear strip theory using retardation functions to obtain a two dimensional time domain solution with second order wave forces, a thrust model and a nonlinear maneuvering model. The outcomes were compared with experimental data of a freely running model.

Mortola et al. (2011) proposed a more complex time domain solution employing a two dimensional nonlinear radiation solution on the actual wetted surface below the undisturbed waves combined with nonlinear restoring and wave exciting forces. They presented a comparison of the proposed method and two and three dimensional linear approaches applied to the S-175 container ship.

For motions and loads of high speed planing craft time domain methods based on two dimensional time domain theory are often applied. Faltinsen and Sun (2011) computed the dynamic response of planing vessels in regular



head seas using a 2D+t methodology. They introduced three dimensional corrections at the transom stern assessing the influence of the flow around the transom on the vertical plane motions.

Rijkens (2013) used a nonlinear semi-empirical strip theory method for high speed craft in an real-time active control scheme for reducing vertical acceleration levels in head waves. Continuous ship response predictions are made based on the incident wave to estimate the vertical acceleration level, leading to interventions by the control system when a threshold value is exceeded by means of thrust reduction or control device actuation.

(ii) 3D transient Green Function Methods

Three dimensional transient Green Function Methods only require panelling of the wetted hull geometry, relying on a linearized free surface boundary condition that is automatically satisfied by the transient Green function, as well as the radiation condition. Typically, the approach used allows for direct incorporation of forward speed effects at the cost of a relatively complicated numerical scheme.

Time domain GFM approaches come in various degrees of complexity, ranging from fully linear time domain approaches that only require setting up the influence matrix once for the entire time domain simulation to body exact approaches that require re-panelling and re-computation of the influence matrix at each time step. There are many intermediate possibilities, by using nonlinear restoring forces and nonlinear Froude-Krylov forces on the actual wetted body. These approaches are often loosely termed 'blended methods' or 'semi-nonlinear methods'.

Datta et al. (2013) used a linear time domain GFM for the analysis of radiation forces on a ship advancing with forced heave and

pitch motions. They compared their outcomes to experimental data and the results obtained with conventional strip theory. They concluded that forward speed has a significant effect on the coupling effects between heave and pitch and stressed the importance of taking into account the linear interactions between steady and unsteady flows.

The application of semi-nonlinear GFM to high speed semi-displacement vessels was studied by van Walree and de Jong (2011) and Hughes and Weems (2011). Van Walree and de Jong validated their body linear time domain method with nonlinear restoring and incident wave forces by deterministically comparing with the motions obtained with model experiments in stern-quartering seas of a fast patrol boat. To achieve this, they reconstructed the wave train from the experiments as an input for their simulations.

Hughes and Weems (2011) used a comparable method (LAMP) with an active ride control system to simulate the motions of a high speed wave piecing catamaran and validated against data obtained from full scale sea trials. They also compared their outcomes with the results of linear frequency domain simulation and stressed the necessity of time domain simulation to enable nonlinear aspects of the ride control system.

A body exact GFM was presented by Zhang et al. (2011) using a more sophisticated version of LAMP. They introduced the pre-corrected Fast Fourier Transform (pFFT) method in their solution scheme to improve computational efficiency in terms of both CPU time and the required core memory for (linear and nonlinear) problems with a very large number of unknowns.

Van Walree and Turner (2013) presented the development and validation of a body exact GFM. Based on the weak scattered assumption,



they transformed hull surface vertically to apply the linear free surface condition in a nonlinear way on the incident wave surface. They validated their results against motions and pressures obtained with model experiments with a patrol boat in head seas. Their method was shown to be able to capture the pressure peaks occurring during slam events.

(iii) 3D time domain Rankine Panel Methods

The Rankine Panel Method (RPM) uses a distribution of singularities of much simpler form compared to the GFM. However, in order to satisfy the free surface condition also panels need to be distributed over the free surface and the radiation condition requires an additional numerical method such as a numerical beach. The distribution of singularities over the free surface enables the relatively easy extension to nonlinear analysis. The RPM has gained significant popularity over the past decade. Also the RPM comes in multiple forms, ranging from fully linear to body exact and a nonlinear free surface condition.

Zaraphonitis et al. (2011) performed seakeeping analysis of a medium speed container vessel with a linear RPM. They also applied linear strip theory and a frequency domain GFM and compared the relative merits of the three computational methods of varying degree of complexity.

Ommani and Faltinsen (2011) applied the linear time domain RPM for the hydrodynamics of semi-displacement vessels. They incorporated transom effects by modeling a hollow behind the transom based on an analytical approach and the unsteady flow is linearized about the steady flow including the hollow. They showed results in good overall agreement with experimental data obtained in literature.

Kim and Kim (2013) combined a linear RPM with a numerical wave tank generating

linear waves and Boussinesq-type shallow water waves to evaluate the influence of nonlinear behaviour. They did not find significant differences between linear and nonlinear waves. They performed an analysis of the hydrodynamic coefficients, wave loads, and motion responses for a LNG carrier and observed the influence of varying bathymetry.

Song et al. (2011) validated a weakly nonlinear RPM consisting of a linear RPM combined with nonlinear restoring and incident wave forces for ship motions and structural loads on a container ship. They recommended that to control the non-restoring horizontal plane motions in steep stern quartering seas they carefully considered soft springs for better computational accuracy.

You and Faltinsen (2012) developed a fully nonlinear RPM combined with a numerical wave tank and numerical damping zone to simulate the interaction between moored floating bodies and waves in six degrees of freedom. After presenting verification and validation results they present a simulation of a moored Wigley hull in regular waves in shallow water.

Xu and Duan (2013) used a multi-transmitting formula with artificial wave speed to eliminate wave reflection on the artificial boundary, demonstrating that their method is capable of performing stable long time simulations of floating bodies. Nan and Vassalos (2012) included the m-terms in the body boundary condition of a RPM with a double body linearization.

(iv) Higher Order Boundary Element Methods (HOBEM)

In higher order BEMs the boundary surfaces are discretized with higher order boundary elements avoiding some of the problems introduced by the stepwise discretization of the



traditional constant panel methods. The higher order elements allow for much smoother representation of the velocity potential and its derivatives and therefore require much less elements compared to traditional panel methods and allowing for much easier evaluation of spatial flow derivatives.

He and Kashiwagi (2013) developed a higher-order BEM within the frame of linear potential flow theory to predict the radiation forces of a Wigley forced heave and pitch at forward speed. They used the Rankine source as the kernel function. The results were compared to model experiments and other numerical solutions.

Shao and Faltinsen (2012) presented an alternative formulation of the boundary value problem in a body-fixed coordinate frame, avoiding the numerical difficulties associated with the m_j -terms and their derivatives. They used a higher order BEM with cubic shape functions as solution scheme. They applied the method to second order sum frequency excitation of ship springing.

(v) *Finite Element Methods*

An alternative to Boundary Element Methods is the application of the Finite Element Method to solve the potential flow problem. Hong and Nam (2010) used a FEM method to analyze second-order wave forces on side-by-side moored floating bodies. Yan and Ma (2011) used the quasi arbitrary Lagrangian-Eulerian Finite Element Method based on fully nonlinear potential flow theory to investigate the nonlinear interaction between two floating structures.

(vi) *Hybrid methods*

Usually hybrid methods consist of a sophisticated inner domain solution matched with a

more efficient outer domain solution. Tong et al. (2013) presented a matched Rankine Panel Method with a Green Function Method in the outer domain.

Kjellberg et al. (2011) developed a nested approach that combines a two-dimensional numerical wave tank with a three-dimensional fully nonlinear body exact boundary element method using constant strength source panels that only resolves the 3D flow in vicinity of the hull.

Guo et al. (2012) presented a coupled numerical wave model using a Volume Of Fluid (VOF) method to resolve the extreme wave motions near a structure while using a BEM further upstream.

Weymouth and Yue (2013) developed physics-based learning models for ship hydrodynamics. This approach uses a very limited amount of high fidelity data points obtained from experiments or CFD computations combined with a large amount of intermediate data points for the same problem obtained from less accurate but far more efficient methods such as linear potential flow methods. The approach then uses both data sets to generate an improved prediction over the entire data range. The aim is to achieve far more accurate simulations, while spending a minimum amount of computational effort.

Maneuvering in Waves and Dynamic Stability

There is a growing interest in the assessment of the dynamic stability of ships operating in waves, due to IMO activity regarding the update of intact stability criteria. This development has led to an increased demand for numerical methods capable of dealing with the problem of a ship maneuvering in waves.



Skejic and Faltinsen (2013) analyzed ship maneuvering in waves by using a unified seakeeping and maneuvering two-time scale model. They used an approximated method for slow drift second order drift forces combined with a maneuvering model based on nonlinear slender body theory.

Yu and Ma (2012) considered a frequency domain strip theory solution transferred to the time domain with nonlinear restoring forces incorporating rudder control and propeller forces. They applied the method to parametric roll of container vessels.

Belenky and Weems (2012) used a linear GFM combined with nonlinear restoring and incident wave forces to determine the interdependence of roll angles and rates. Van Walree (2012) used a very similar approach for the behaviour of a destroyer in steep stern-quartering seas.

Kim and Sung (2012) extended a nonlinear time domain seakeeping panel method by adding resistance, propulsion and maneuvering force models. They calibrated the maneuvering force model with captive model tests and carried out numerical simulations for a container vessel in waves.

2.2.3. Rarely Occurring Events

Slamming

Slamming is defined as an impact between the hull of a vessel and the water surface. Keel, stern, flare or wet deck slamming can impart significant global and local structural loads onto vessels. The impacts can also induce vibration within the ship (known as whipping) and can ultimately lead to an increase in structural fatigue.

Developing techniques to accurately predict the magnitude of slamming events is still a key focus for researchers. Yang et al. (2013) presented a technique to estimate slamming impact loads and dynamic structural responses of containerships at an initial design stage using a direct analysis method based on fluid-structure interaction. The method is based on using a commercial CFD program (STAR-CCM+) and a structural analysis program (ABAQUS), respectively. Bow and stern slamming loads were calculated, but the authors undertook no validation. Rahaman and Akimoto (2012) used a RANS based motion simulator to model slamming of a modern container ship. The numerical method was successfully validated in regular head waves and mechanism of slamming on the bow flare region analyzed based on visualization of flow field.

Full-scale measurements are an extremely effective mechanism for investigating slamming behavior, although they are complex and expensive to conduct. Ogawa et al. (2012) examined the relationship between the occurrence probability of a slamming induced vibration and sea state based on the full-scale measurement data of two large container ships.

Jacobi et al. (2014) investigated the slamming behaviour of a 98m high-speed catamaran through the analysis of extensive full-scale trials data. Slam occurrence rates were found for a range of conditions and the influence of vessel speed, wave environment and heading determined. Since the ship was equipped with a ride control system its influence on the slam occurrence rates was also assessed. Identifying slam events in full-scale trials data can be challenging; however Amin et al. (2012) introduced, described, applied and recommended the continuous wavelet transform as an effective means to identify and investigate the wave induced hull vibrations in both the time and frequency domains simultaneously.



Using experimental data for a hydroelastic model of a high-speed ferry, Dessi and Chiappi (2013) analyzed the statistical properties of the slamming impact process. One of their major findings was that the impact statistics are largely affected by the grouping of slams into clusters, thus violating the hypothesis of mutual independence between successive impacts that is at the basis of most of the statistical models. They also proposed a new criterion for slamming identification based on the evaluation of the whipping bending moment.

Chen et al. (2012) having performed model experiments on a segmented hydroelastic model concluded that in larger sea states the influence of whipping has a major influence on the magnitude of the longitudinal bending moment. They also found that a linear hydroelastic theory can accurately predict the bending moment in small sea states.

A hydroelastic model was used by Lavroff et al. (2013) and French et al. (2013, 2014) to examine the slamming behaviour of large high speed catamarans. Lavroff et al. (2013) performed towing tank tests in regular seas to measure the dynamic slam loads acting on the centre bow and vertical bending moments acting on the demihulls of the catamaran model as a function of wave frequency and wave height. Peak slam loads measured on the centre bow of the model were found to approach the total mass of the model. French et al. (2013, 2014) investigated slamming behaviour in irregular waves finding that encounter wave frequency and significant wave height are important parameters with regard to centrebow slamming, but that relative vertical velocity is a poor indicator of slam magnitude.

Water Entry

The ability to accurately predict the loads and pressures on a body entering the water is fundamental to the slamming problem.

Korobkin (2011, 2013) continues to work on this fundamental problem. Korobkin (2011) presented a numerical method to solve the problem of symmetric rigid contour entering water at a given speed based upon the so-called Generalized Wagner Model (GWM). The solution derived predicts accurately the hydrodynamic force similar to Modified Logvinovich Model (MLM) but additionally it gives access to the pressure distribution, which is not available within MLM. This method was extended by Korobkin (2013) to accurately account for the second stage of the flow, when the wedge is already completely wetted and a cavity is formed behind the wedge.

Drop tests provide the ability to obtain experimental results for the water entry problem. Alaoui et al. (2012) conducted drop tests on cones (with and without knuckles) and hemispheres at constant velocity. The experimental set up enabled impacts at high-speeds with small velocity deviations. Good agreement between numerical results using Impact++ ABAQUS, ABAQUS/Explicit and FLUENT codes and available experimental measurements were obtained.

Panciroli (2012) conducted a series of drop test experiments on flexible wedges and found that large structural deformations generate two fluid-structure interaction phenomena that never occur in rigid-bodies impact: (i) the repetition of impacts and separation between the fluid and the structure in the region characterized by the fluid jet generated during the water entry and (ii) an underpressure region with a cylindrical wavefront in the underwater fluid/structure interface. Yamada et al. (2012) used LS-DYNA whereby the fluid structure



interaction (FSI) is taken into account by coupling fluid analysis and structural analysis in each time step of time domain simulations. Comparisons were made of the pressure distribution and slamming impact water entry of a rigid wedge, with those determined by conventional Wagner theory.

Reynolds-Averaged Navier-Stokes Equations (RANSE) appear to be able to satisfactorily model the water entry problem. Swidan et al. (2013) used quasi-2D drop test experimental measurements to validate the simulation of symmetric wedge water impacts using RANSE, with close agreement found between the experimental and numerical results.

Green Water

Green water on deck can result in significant loads that are significant with respect to the safety of forward stowed cargo and deck equipment. Kim et al. (2013) provided an analysis procedure to calculate the design pressure on ship's breakwaters using the Computational Fluid Dynamics (CFD) method and provided the technical background of the newly proposed rule requirements for breakwaters. Zhang et al. (2013) used a Moving Particle Semi-implicit (MPS) method to simulate green water on deck scenarios and successfully validated the technique with experimental data available in the literature. A similar MPS method was used by Bellizi et al. (2013) to investigate the effect of bow shape on green water on deck.

Buchner and van den Berg (2013) studied green water on deck emanating from the side of the vessel using experiments. They concluded that this is a very complex process that will need CFD for the prediction of important non-linear effects. Their model tests can be used as important validation material in this process.

Extreme Accelerations on Small High-Speed Craft

When operating in waves, small high-speed craft can experience extreme accelerations if the hull exits the water and slams upon re-entry. Modelling the wave impacts is a current industry challenge and as such Rose et al. (2011) used a vibro-impact oscillator to model non-linear planing hull accelerations and predict extreme events in variable environments. Whilst Riley et al. (2011) presented a simplified approach to quantifying the comparison of acceleration responses of small high-speed craft in rough seas and proposed the use of a Ride Quality Index (RQI).

An effective method of reducing the likelihood of these extreme events is through a ride control system. Rijkens et al. (2011) developed a computational tool for the design and optimisation of these ride control systems for high speed planing monohulls. Hydrodynamic characteristics of both transom flaps and interceptors were determined by a systematic series of model test experiments.

2.2.4. Hydroelasticity

Understanding the hydroelastic response of a ship is an important part of the overall structural response. This is true for both extreme ship structural responses and the fatigue loads of some structural details. The challenges are both in model test techniques as well as development and verification/validation of numerical methods. The applicability of the methods for design applications are also addressed.

K.-H. Kim et al. (2013) presented a fully coupled BEM-FEM analysis for ship hydroelasticity in waves. For the analysis of fluid-structure interaction problems, a partitioned method was applied. The fluid domain surrounding a flexible body was solved using a B-spline Rankine panel method, and the structural



domain was handled with a three-dimensional finite element method. The two distinct methods were fully coupled in the time domain. The numerical results of natural frequency and the motion responses of simple and segmented barges were computed to validate the method. The study extended to the application to two real ships, 6500 TEU and 10,000 TEU container ships, for more validation and also observation on the practicality of the method. It was found that the method provides reliable solutions to linear ship hydroelasticity problems.

J.-H. Kim et al. (2013a) introduced an analysis of ship hydroelasticity for a fatigue assessment of ship structural design. In this study, the hydroelastic analysis for springing and whipping was carried out by using a fully coupled three-dimensional BEM-FEM approach with two-dimensional slamming theories, and a sequential fatigue assessment is performed. The fatigue damage was decomposed to wave frequency and high frequency components. Furthermore, the high frequency component was again decomposed to 1st harmonic springing, super harmonic springing and whipping contributions. The amount of the contributions was compared in irregular sea states.

J.-H. Kim et al. (2013b) applied different numerical methods for the coupled hydroelasticity analysis of ship structures in regular and irregular waves. For the hydrodynamic analysis of flexible body motion, a time domain Rankine panel method was applied. For the structural analysis, three different approaches were considered: beam approximation, modal approach by using the eigenvectors of three-dimensional (3-D) finite element (FE) model, and full 3-D FE analysis. For the computation of slamming force, wedge approximation and generalized Wagner model (GWM) were applied for 2-D slices of the ship. The computational results were compared with experimental results for the validation of the methodology

and numerical scheme. The hydroelastic motions and loads on ship structures were compared for segmented models of large container ships.

He and Kashiwagi (2012) developed a hydroelastic simulation method based on BEM with MEL for fully nonlinear water waves and FEM for elastic deflection. A hybrid wave-absorbing beach was installed to prevent wave reflection from the end of the wave tank. Using this simulation method, they simulated the interaction of a surface-piercing plate with non-zero initial free surface and compared the result with the corresponding linear analytical solution. They also simulated hydroelastic response of a surface-piercing vertical plate due to a solitary wave.

Das and Cheung (2011) proposed a hydroelasticity model to couple the hydrodynamic load, elastic deformation, and rigid-body motion for marine vessels advancing in ocean waves. Small amplitude assumptions of the surface waves and body surface motions lead to linearization of the mathematical problem in the frequency domain. The formulation adopted a translating coordinate system with the free surface boundary conditions accounting for the double body flow around the vessel and the radiation condition taking into account the Doppler shift of the wave field. A boundary element model, based on the Rankine source distribution, described the potential flow and the hydrodynamic pressure on the vessel. A finite element model relates the hull motion to the hydrodynamic pressure through a kinematic and a dynamic boundary condition. This direct coupling of the structural and hydrodynamic systems leads to a matrix equation in terms of the body surface displacement. The model was verified with published data from the modal superposition method without forward speed effects and applied to examine the characteris-



tics of a flexible Wigley hull advancing in waves.

Piro and Maki (2011) studied hydroelastic impact together with the exit of simple ship sections. The method used a loosely coupled fluid-structure interaction (FSI) solver to couple a finite element model to a computational fluid dynamics (CFD) model. The structure was represented using beam and plate finite elements and decomposed into its dry mode shapes. The motion of the structure was applied to the boundary of the CFD simulation using either the exact or approximate body boundary condition. The fluid pressure on the structure was expanded in the structural modes and applied in the force term of the structural equations of motion. The system was solved iteratively in each time step to ensure time accuracy. The hydroelastic impact of a wedge was studied to validate the numerical method and the exit of the wedge from the water was investigated.

Paredes and Imas (2011) investigated the three-dimensional fluid-structure interaction between a free-surface disturbance and a deformable membrane as a canonical problem representative of the interaction between a surface-effect ship (skirt) advancing with forward speed in waves. The numerical study was performed using a hydrodynamic solver developed around an SPH algorithm that was used to simultaneously model both the fluid dynamics and structural dynamics with two-way fluid-structure coupling. Results from this study were presented along with validation examples and as well as a discussion of their SPH algorithm, in particular their methodology for treatment of boundary conditions, FSI, and fluid viscous effects.

Iijima et al. (2011) evaluated the effect of the wave-induced vibrations on long-term fatigue damage in various types of ships is evaluated by using a series of numerical simulations.

A bulk carrier, a VLCC, and a container carrier were employed as subject ships. A fully three dimensional numerical method was employed for evaluating the load effects. The pressure obtained by three-dimensional potential theory was integrated over the instantaneous wet surface to account for linear and nonlinear wave loads. Slamming loads were separately modelled by using momentum theory. The calculations were performed for the respective short-term sea states. The characteristics of the fatigue damage by the wave-induced vibrations were clarified. It was shown that the amount of the increase in fatigue damage depends on the wave loading properties of the ships in waves as well as the structural properties such as natural frequencies of flexible modes.

Stenius et al. (2011) discussed challenges in modeling and quantifying hydroelastic effects in panel-water impacts and summarised results from numerical and experimental studies. Kinematic and inertia related hydroelastic effects were discussed and exemplified in relation to pressure distributions and structural responses. Hydroelastic effects were quantified by comparing hydroelastic results with rigid/quasi-static reference results. The formulation of non-coupled reference solutions in experimental studies is particularly challenging and the paper addressed this problem by outlining a semi-empirical approach to reach such solutions. For those impact situations where the hydroelastic interaction seemed to have a significant effect, it was found both numerically and experimentally that the hydroelastic effects were amplifying the structural responses in comparison to the rigid/quasi-static reference solutions. Two approaches for characterization of impact situations regarding the involved hydroelastic effects in relation to panel properties and impact conditions were discussed and exemplified. These approaches can tentatively be used to evaluate the hydroelastic effects in design situations.



White et al. (2012) presented some methods to determine values of dynamic bending moments considering the effects due to whipping and springing which are suitable for design application. Examples of the use of these methods were also presented.

Senjanović et al. (2011, 2013) discussed treatment of the restoring stiffness, which couples displacements and deformations, playing a very important role in hydroelastic analysis of marine structures. The problem of its formulation is quite complex and is still discussed in relevant literature. Different numerical formulations were implemented and compared.

Begovic et al. (2011) presented an experimental investigation to obtain motion and load measurements of an intact and damaged frigate model in waves. The experimental measurements showed the changes in motion and hull girder loading when a ship hull is damaged. The obtained data were compared with numerical predictions from non-linear time domain motion code (strip theory) implemented in ShipX.

Chen et al. (2012) carried out segmented ship model experiments on bow slamming and whipping of a ship. A nonlinear hydroelasticity method considering slamming loads was proposed. Variable cross-section beams were used to improve the simulation of the stiffness of the hull. Severe bow slamming was observed when the model was in head-following regular waves. Experimental results showed that when the wave height increased from 5.6m to 21m the mean value of the total moment increased from 25% to 92% compared with that of the wave moment because of severe whipping. The measured results on the central hull in different sea states were compared with calculations based on linear and nonlinear hydroelasticity theory showing that their present

method and program can predict the wave loads properly.

Matsubara et al. (2011) performed model tests on a segmented model of a wave-piercing catamaran to obtain experimental values of global motions and loads as well as slamming loads, with a particular focus on the influence of the centrebow configuration. The motions were found to be distinctly non-linear with respect to wave height; this was due to the immersion of the centrebow in larger waves tending to reduce the heave and pitch motions. The wave loads were found to be dominated by the slam load on the centrebow, varying in magnitude and location with respect to wave conditions.

Wu and Stambaugh (2013) presented a comparative study carried out for a 45m long high-speed vessel. The time history of the vertical bending moments (VBM) and the standard deviations of both wave-frequency and high-frequency components in the VBM were compared between model tests and numerical simulations. A comparison of the probability of exceedance derived from the hydroelastic hogging and sagging vertical bending moments was also presented. Different aspects of model testing and numerical simulation were discussed. The paper concludes that an integrated approach, that uses the advantages of both model testing and numerical simulation while overcoming the drawbacks of either method applied alone, is the best way forward in the near future.

Halswell et al. (2011) discussed each area of hydroelasticity found in an inflatable boat; defining each problem and possible methods of investigation. Anecdotal evidence has shown that this flexibility or hydroelasticity of an inflatable boat improves its performance, especially in waves.



Besten et al. (2011) developed an analytical, 2D, mathematical model for the local structural response of a hydrodynamic impact loaded sandwich structure with vibration isolation and structural damping properties. The structural response was determined by solving semi-analytically a hydro-elastic coupled sandwich flexible core model and a hydrodynamic impact model in modal space, verified by results found in literature and FEM calculations.

3. PROCESS FOR THE ESTIMATION OF SHIP SPEED REDUCTION COEFFICIENT f_w IN WAVES

3.1. Introduction

The speed reduction coefficient f_w is introduced in the 2012 Guidelines on the method of calculation of the attained energy efficiency design index for new ships (EEDI), adopted by MEPC.212(63). f_w is a non-dimensional coefficient indicating the ship speed reduction in a representative sea condition of wave height, wave frequency and wind speed. As the representative sea condition, Beaufort scale 6 was adopted by MEPC considering mean sea condition of north Atlantic and north Pacific. f_w can be determined by conducting the ship specific simulation on its performance at representative sea condition.

In the following review of the state of the art for the f_w estimation process, ship resistance as well as brake power in a calm sea condition (no wind and no waves) is assumed to be evaluated by tank tests, which means model towing tests, model self-propulsion tests and model propeller open water tests. Numerical calculations can be used as equivalent to model propeller open water tests or used to complement the tank tests conducted to evaluate the

effect of additional hull features such as fins, etc., on ship's performance.

For the estimation of f_w to evaluate EEDI, the design parameters and the assumed conditions in the simulation to obtain the coefficient f_w should be consistent with those used in calculating the other components in the EEDI.

3.2. Basic Conditions in the Prediction of Ship Speed Reduction

Symbols for ship performance (also refer to Figures 19 and 20)

P_B : Brake power

R_T : Total resistance in a calm sea condition (no wind and no waves)

V_{ref} : Design ship speed when the ship is in operation in a calm sea condition (no wind and no waves)

V_w : Design ship speed when the ship is in operation under the representative sea condition

ΔR_{wave} : Added resistance due to waves

ΔR_{wind} : Added resistance due to wind

η_D : Propulsion efficiency

η_S : Transmission efficiency

Subscript w refers to wind and wave sea conditions.

Symbols for representative sea conditions

D : Angular distribution function

E : Directional spectrum

H : Significant wave height

S : Frequency spectrum

T : Mean wave period

α : Angle between ship course and regular waves (angle 0(deg.) is defined as the head waves direction)



θ : Mean wave direction ($\theta = 0$ (deg.))
 ω : Circular frequency of incident regular waves

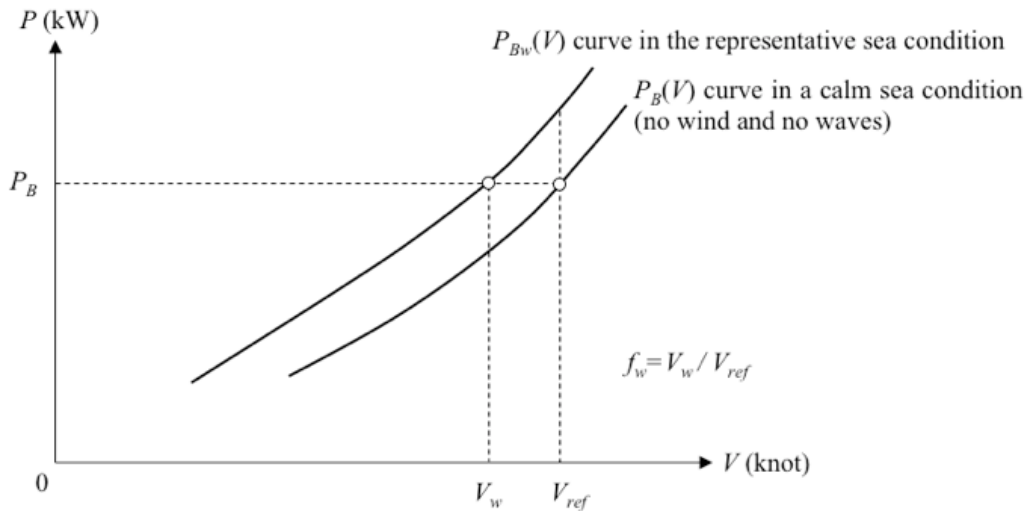


Figure 19. Relationship between power and ship speed reduction.

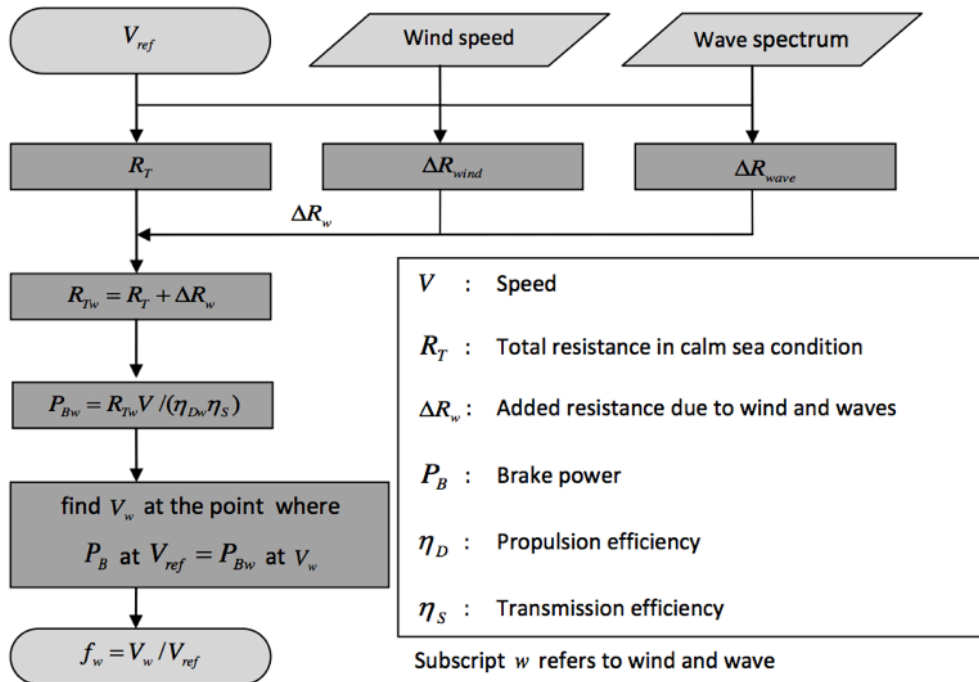


Figure 20. Flow chart of the calculation of ship speed reduction

The representative sea conditions for ships have to be determined first. The sea condition for the prediction of ship speed reduction is

dependent on marine area. Larger ships are operated in relatively shorter wave length and lower wave height waves than smaller ships.



Therefore, even in the same sea condition, ship speed reduction can be dependent on ship dimension, i.e. capacity of cargo, and ship type. The direction of wind and waves are defined as heading direction, which has the most significant effect on the speed reduction. As ocean waves are characterised as irregular, the directional spectrum should be considered. To obtain the mean wave period from the Beaufort scale, the following formula derived from a frequency spectrum for fully-developed waves is used.

$$T = 3.86\sqrt{H} \quad (1)$$

where H is the significant wave height in metres and T is the mean wave period in seconds.

The directional spectrum E is composed of frequency spectrum S and angular distribution function D .

$$E(\omega, \alpha; H, T, \theta) = S(\omega; H, T)D(\alpha; \theta) \quad (2)$$

$$S(\omega; H, T) = \frac{A_s}{\omega^5} e^{-\frac{B_s}{\omega^4}} \quad (3)$$

where

$$A_s = \frac{H^2}{4\pi} \left(\frac{2\pi}{T_z} \right)^4, \quad B_s = \frac{1}{\pi} \left(\frac{2\pi}{T_z} \right)^4, \quad T_z = 0.920T, \quad (4)$$

$$D(\alpha, \theta) = \begin{cases} \frac{2}{\pi} \cos^2(\theta - \alpha) & \left(|\theta - \alpha| \leq \frac{\pi}{2} \right) \\ 0 & \text{(others)} \end{cases}$$

Ships are assumed to be in steady navigating conditions on a fixed course with constant main engine output. The current effect is not considered.

The total resistance in the representative sea condition, R_{Tw} , is calculated by adding the added resistance due to wind and waves ΔR_w to the total resistance in a calm sea condition R_T . The ship speed V_w is the value of V

where the brake power in the representative sea condition P_{Bw} equals to P_B , which is the brake power required for achieving the speed of V_{ref} in a calm sea condition. Where P_{Bw} can be derived from the total resistance in the representative sea condition R_{Tw} , the properties for propellers and propulsion efficiency η_D should be derived from the formulas obtained from tank tests or an alternative method equivalent in terms of accuracy, and transmission efficiency η_S should be the proven value as verifiable as possible. The brake power can also be obtained from the reliable self-propulsion tests.

$$P_B = R_T V / (\eta_D \eta_S) \quad (5)$$

The coefficient of the ship speed reduction f_w is calculated by

$$f_w = V_w / V_{ref} \quad (6)$$

at the point where

$$P_B \text{ at } V_{ref} = P_{Bw} \text{ at } V_w. \quad (7)$$

Total Resistance In A Calm Sea Condition:

R_T The total resistance in a calm sea condition (no wind and no waves) is evaluated by tank tests, which means model towing tests, model self-propulsion tests and model propeller open water tests. Numerical calculations may be accepted as equivalent to model propeller open water tests or used to complement the tank tests conducted (e.g. to evaluate the effect of additional hull features such as fins, etc., on ship's performance).

Total resistance in the representative sea condition: R_{Tw}

The total resistance in the representative sea condition, R_{Tw} , is calculated by adding ΔR_{wind} , which is the added resistance due to wind, and ΔR_{wave} , which is the added



resistance due to waves, to the total resistance in a calm sea condition R_T .

$$\begin{aligned} R_{Tw} &= R_T + \Delta R_w \\ &= R_T + \Delta R_{wind} + \Delta R_{wave} \end{aligned} \quad (8)$$

Added resistance due to wind: ΔR_{wind} . Added resistance due to wind can be calculated by the following typical formula on the basis of the mean wind speed and wind direction.

$$\Delta R_{wind} = \frac{1}{2} \rho_a A_T C_{Dwind} \left\{ (U_{wind} + V_w)^2 - V_{ref}^2 \right\} \quad (9)$$

C_{Dwind} should be calculated by a formula with considerable accuracy, which has been confirmed by model tests in wind tunnel. More general formula can be applied when wind direction is not longitudinal, e.g. Fujiwara and Ueno (2006), Blendermann (1994). The vertical profile of wind can be also considered. There are a few different models of vertical variation for ocean waves such as models based on power law (Blendermann, 1994) and logarithmic approximation (DNV, 2010). These models can be applied for the more accurate prediction of C_{Dwind} .

Added resistance due to waves: ΔR_{wave} . Irregular waves can be represented as linear superposition of the components of regular waves. Therefore added resistance due to waves is also calculated by linear superposition of the directional spectrum E and added resistance in regular wave.

$$\Delta R_{wave} = 2 \int_0^{2\pi} \int_0^\infty \frac{R_{wave}(\omega, \alpha; V)}{\zeta_a^2} E(\omega, \alpha; H, T, \theta) d\omega d\alpha \quad (9)$$

Added resistance in irregular waves R_{wave} should be determined by tank tests or a formula equivalent in terms of accuracy. In cases of applying the theoretical formula, added resistance in regular waves, R_{wave} , is calculated from the radiation and diffraction components of added resistance primary induced by ship motion and wave diffraction in regular waves, R_{wm} , and the reflection component due to wave reflection for the correction of added resistance in short waves, R_{wr} .

$$R_{wave} = R_{wm} + R_{wr} \quad (10)$$



Table 4. Methods for added resistance prediction

Approaches	Numerical method			Experiment
	Slender-body theory	3D panel method	CFD	
Added resistance computation	Direct pressure integration (e.g. Faltinsen et al, 1980, Kim & Kim, 2011)		Direct pressure integration: Added resistance = (Total Resistance in waves) – (Resistance in cal water)	
	Momentum conservation method (e.g. Maruo, 1960, Joncquez, 2009)			
	Radiated energy method (e.g. Salvesen, 1978)			
Methodology	Strip method, (enhanced) unified theory	Green-function method, Rankine panel method	Commercial or in-house codes	Surge-fixed or surge-free tests
	Linear formulation for seakeeping.		Fully nonlinear formulation.	Fully nonlinear
Short-Wave Approximation	Faltinsen's approximation, NMRI's empirical formula			
Remarks	Quick computation	Different formulations for time-domain and frequency-domain methods.	A lot of computational time	Expensive
	In short waves, empirical or asymptotic formula should be combined.	Grid dependency should be observed in short waves.	Strong grid dependency in short waves.	Scale dependency and repeatability should be observed.

3.3. Calculation Methods for Added Resistance in Regular Waves

Added resistance can be obtained either by using numerical computation or towing-tank experiments. Since added resistance is the second-order mean quantity which can be obtained by linear solution of the seakeeping problem, linear seakeeping programs can be applied. The method of added resistance prediction in regular waves can be summarized as in Table 4. The comparison of added resistance obtained by different methods has been recently introduced by Seo et al. (2013).

3.4. Correction of added resistance in short waves, R_{wr} .

Symbols

B : Ship breadth

B_f : Bluntness coefficient, which is derived from the shape of water plane and wave direction

β : Wave incident angle (defined in Figure 19)

C_U : Coefficient of advance speed, which is determined on the basis of the guidance for tank tests



- d : Ship draft
 $F_n = V/\sqrt{L_{pp}g}$: Froude number (non-dimensional number in relation to ship speed)
 g : Gravitational acceleration
 I_1 : Modified Bessel function of the first kind of order 1
 k : Wave number of regular waves
 K_1 : Modified Bessel function of the second kind of order 1
 ζ_i : Incident wave elevation
 $\bar{n} = (n_1, n_2, n_3)$: Normal vector on ship surface
 L : Ship length
 ρ : Water density
 U : Ship speed
 (x_0, y_0) : Position of body surface
 ω_e : Encounter wave frequency

To overcome the difficulty of computing added resistance in short waves several formulae can be used:

Ray theory formulation: Faltinsen et al. (1980)

The integration in Eq. (11) is performed over the non-shaded part (A-F-B) of the waterline as shown in Figure 21.

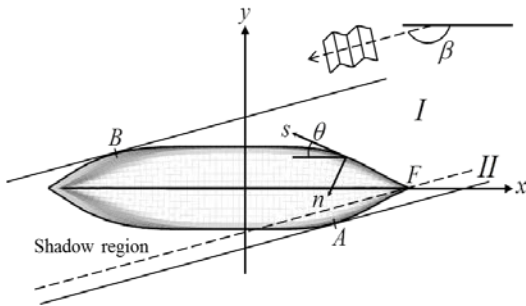


Figure 21. Coordinate system for the added resistance calculation in the short wave range

$$\begin{aligned}
 R_{wave} &= \frac{1}{2} \rho g \zeta_i^2 \\
 &\times \int_L \left[\sin^2(\theta - \beta) + \frac{2\omega U}{g} [1 + \cos \theta \cos(\theta - \beta)] \right] \bar{n} dl \\
 (n_1 = \sin \theta, \quad n_2 = \cos \theta, \quad n_3 = x_0 \cos \theta - y_0 \sin \theta)
 \end{aligned} \quad (11)$$

Semi-empirical formulae

$$R_{wave} = \alpha_d (1 + \alpha_U) \left[\frac{1}{2} \rho g \zeta_i^2 BB_f(\beta) \right] \quad (12)$$

where

$$B_f(\beta) = \frac{1}{B} \left[\int_I \sin^2(\theta - \beta) \sin \theta dl + \int_{II} \sin^2(\theta + \beta) \sin \theta dl \right] \quad (13)$$

- Fujii and Takahashi (1975)

$$\alpha_d = \frac{\pi^2 I_1^2(kd)}{\pi^2 I_1^2(kd) + K_1^2(kd)}, \quad 1 + \alpha_U = 1 + 5\sqrt{F_n} \quad (14)$$

- NMRI (Tsujiimoto et al. 2008, Kuroda et al. 2008)

Added resistance in regular waves for correcting R_{wm} is calculated as follows.

$$R_{wr} = \frac{1}{2} \rho g \zeta_a^2 BB_f (1 + C_U F_n) \alpha_d \quad (15)$$

where

$$\begin{aligned}
 \alpha_d &= \frac{\pi^2 I_1^2(K_e d)}{\pi^2 I_1^2(K_e d) + K_1^2(K_e d)}, \\
 K_e &= K(1 + \Omega \cos \alpha)^2, \quad \Omega = \frac{\omega V}{g},
 \end{aligned}$$

$$\begin{aligned}
 B_f(\beta) &= \frac{1}{B} \left[\int_I \sin^2(\theta - \beta) \sin \theta dl \right. \\
 &\quad \left. + \int_{II} \sin^2(\theta + \beta) \sin \theta dl \right]
 \end{aligned}$$

dl is a line element along the water plane, β_w is the slope of line element along the waterline, and domains of integration are shown in Figure 22. Unified definition of the heading angle of



ship to wind and wave is used to prevent confusion in MEPC, i.e. $\alpha = 0$ for head sea.

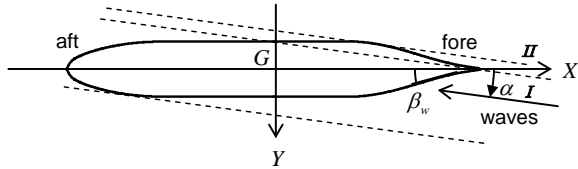


Figure 22. Coordinate system for R_{wr}

Effect of advance speed α_U is determined as follows:

$$\alpha_U = C_U(\alpha)F_n \quad (16)$$

The coefficient of advance speed in oblique waves $C_U(\alpha)$ is calculated as follows:

$$C_U(\alpha) = \text{Max}[F_S, F_C] \quad (17)$$

where

- (i) $B_f(\alpha = 0) < B_{fc}$ or $B_f(\alpha = 0) < B_{fs}$:
- $$F_S = C_U(\alpha = 0) - 310\{B_f(\alpha) - B_f(\alpha = 0)\},$$
- $$F_C = \text{Min}[C_U(\alpha = 0), 10]$$
- (ii) $B_f(\alpha = 0) \geq B_{fc}$ and $B_f(\alpha = 0) \geq B_{fs}$:
- $$F_S = 68 - 310B_f(\alpha), \quad F_C = C_U(\alpha = 0)$$
- and $B_{fc} = \frac{58}{310}$, $B_{fs} = \frac{68 - C_U(\alpha = 0)}{310}$.

3.5. A Practical Estimation of f_w from Standard Curve

The design parameters in the calculation of f_w from the standard f_w curves should be consistent with those used in the calculation of the other components in the EEDI. Three kinds of standard f_w curves are provided for bulk carriers, tankers and containerships, and expressed as a function of *Capacity* defined in the 2012

Guidelines on the method of calculation of the attained Energy Efficiency Design Index for new ships (EEDI), adopted by MEPC.212(63). Ship types are defined in regulation 2 in Annex VI to the International Convention for the Prevention of Pollution from Ships, 1973, as modified by the Protocol of 1978, as amended by resolution MEPC.203(62).

The Japanese delegation suggested a method to estimate the coefficient f_w from the standard f_w curves. When real ship data for speed reduction are known, this method can be an alternative method, which does not require computation or experiment. When this is the case, the accuracy of real ship measurement is essential. Otherwise, this approach can provide inaccurate prediction of the coefficient f_w .

Example

Each standard f_w curve has been obtained on the basis of data of actual speed reduction of existing ships under the representative sea condition in accordance with procedure for deriving standard f_w curves. Each standard f_w curve is shown from Figure 23 to Figure 25, and the standard f_w value is expressed as follows:

$$f_w = a \times \ln(\text{Capacity}) + b \quad (18)$$

where a and b are the parameters given in Table 5.

Table 5. Parameters for determination of standard f_w value

Ship type	a	b
Bulk carrier	0.0429	0.294
Tanker	0.0238	0.526
Containership	0.0208	0.633

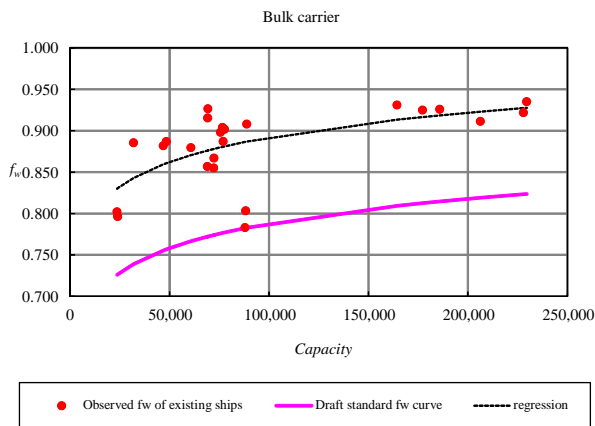


Figure 23. Standard f_w curve for bulk carrier

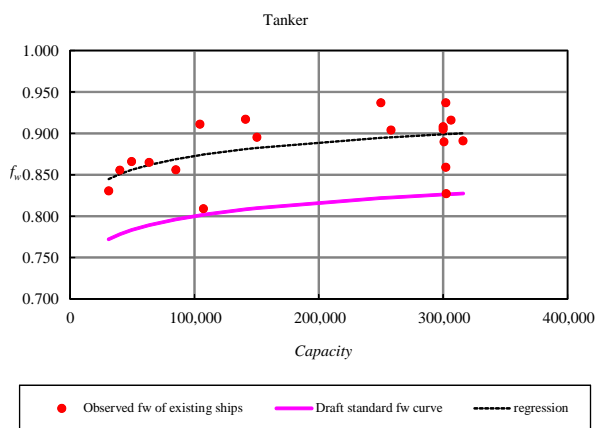


Figure 24. Standard f_w curve for tanker

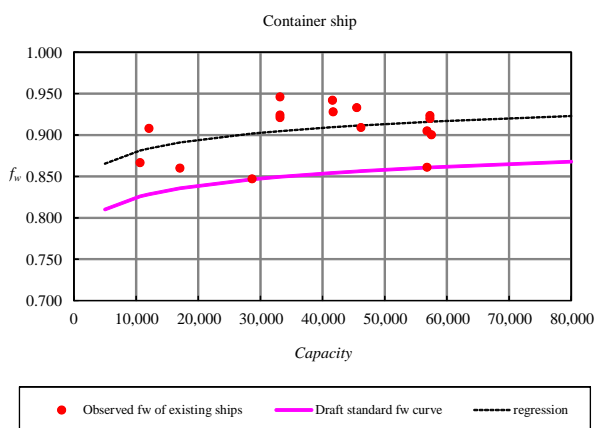


Figure 25. Standard f_w curve for container ship

4. CFD-BASED ANALYSIS ON SEAKEEPING PROBLEMS : STATE OF THE ART REVIEW AND SUMMARY OF METHODOLOGY

During the past two decades, thanks to the rapid development of computer power, computational fluid dynamics (CFD) has been applied to some seakeeping problems. In the broadest sense, ‘CFD method’ refers to all computational methods for fluid flow, including boundary element methods (BEM), finite element methods (FEM), finite difference, or volume, methods (FDM/FVM), spectral methods, etc. However, it is now generally understood that the term ‘CFD method’ concerns only the field equations, i.e. the continuity equation and the Navier-Stokes, or the Euler equation. There are several criteria for the taxonomy of CFD based methods for seakeeping analysis as follows:

- Grid system: grid based method (FDM, FVM, FEM) vs. particle method (SPH, MPS)
- Characteristics of flow I: inviscid vs. viscous (RANS, LES)
- Characteristics of flow II: incompressible (SIMPLE, fractional step) vs. compressible (artificial compressibility)
- Treatment for interface: interface tracking vs. interface capturing (VOF, Level-Set)
- Treatment for moving body: boundary-fitted (re-mesh, overlapping) vs. immersed boundary
- Domain of problem : global flow vs. local flow

This is graphically summarised in Figure 26.

Current numerical methods can be categorised largely into two groups: grid methods and gridless methods. The former is known as an Eulerian approach, which discretizes a fluid volume in structured or unstructured grids and solve the field equations defined on these spatial grids. On the other hand, gridless methods



have seen increased applications recently. These methods, e.g. SPH (smoothed particle hydrodynamics) and MPS (moving particle semi-implicit method), define a finite number of fluid mass (basically, they are volume fractions) and solve the field equations by using their interactions.

In most cases in classical seakeeping problems the effects of viscosity are limited to roll motions or flow around appendages. That is, most problems related to free surface flows in seakeeping problems are inertia-dominant problems and therefore diffusion effects are

relatively smaller than convection effects. In fact, this is the reason why potential flow theory is valid in the ship motion problem and is capable of reasonable accuracy. In many cases, the more important physical phenomenon is the interaction between the free surface flow and air flow. This is the case particularly when the hydrodynamic pressure due to local impacts is of primary interest. As the related problems of ship propulsion, or manoeuvring, in waves become of more interest then the importance of viscous effects will increase in comparison to classical seakeeping problems.

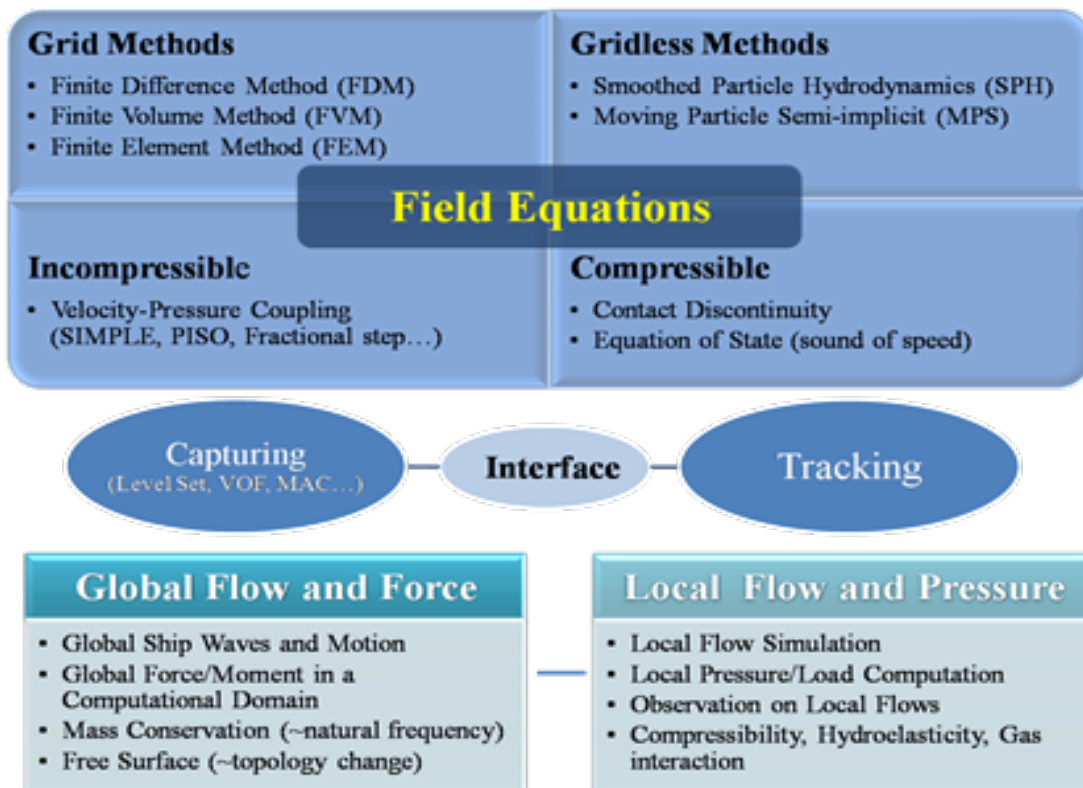


Figure 26. Overall status of the art of CFD schemes: Field equation solvers



Table 6. Summary of CFD methodology for seakeeping analysis

	C. Hu et al. (Kyushu Univ.)	D.G. Dommermut h et al. (SAIC)	J. Yang et al. (Univ. of Iowa)	P. Queutey et al. (ECN)	R. Löhner et al. (George Mason Univ.)	H. Miyata et al. (Univ. of Tokyo)	Y. Kim et al. (Seoul National Univ.)
Discretization for convective term	CIP	3 rd QUICK	3 rd QUICK / WENO	Improved Gamma	Galerkin	QUICK	MC Limiter
Body motion	IBM Particle	IBM Triangle panel	IBM Triangle panel	Mesh Deformation	ALE	Overlapping Grid	IBM Triangle panel
Free surface	THINC (VOF)	CLSVOF	CLSVOF	VOF	VOF	Density Function (QUICK)	THINC (VOF)
Remark		LES	LES Ghost Fluid Method	RANS		RANS	

The key technology in the application of CFD methods to seakeeping problems, including ship motion and local free-surface flows, is how to obtain or trace the dynamic free-surface profile. When grid methods are applied, there are several candidates to choose for the implementation of dynamic and kinematic free-surface boundary conditions. For ship motion problems, VOF (Volume of Fluid) and level-set approaches are popular, but there has also been recent work done using other methods. A good example is CIP (constrained interpolation profile) method. In contrast to grid methods, the numerical treatment of the free surface in particle methods is more straightforward. Most of them adopt a Lagrangian method, i.e. particle tracking with time-marching. Along with the simulation of particle motions inside a fluid volume, particle movement on the free surface can be used to trace its profile. At present commercial programs and the open source program OpenFOAM are commonly applied and it is likely that the application of these programs will be more popular in the future.

The main reason for applying a CFD based method, as opposed to potential flow, to seakeeping analysis is for calculation of problems which contain strongly nonlinear phenomena such as breaking waves, large-amplitude ship motions and wake flows, etc. Besides the accuracy of physical modeling and computational results, the colourful post-processing of results and capability of simulating strongly nonlinear free surface flows are appealing to researchers and engineers. Up-to-date numerical methods such as volume-of-fluid (VOF), level-set methods or particle methods provide reliable results even for the violent flow problem in which the topology of the free-surface boundary is largely distorted, fragmented and merged. Recent turbulence modeling such as RANS and LES become quite popular and they provide reasonable numerical results for an engineering purpose. The major difficulty in the numerical simulation of strongly nonlinear wave-body interaction problems using a field equation solver is that a rigid body can move arbitrarily without coincidence of the grid lines and body boundary, so that

some special treatment is required, such as re-meshing, moving mesh or embedded (overset) meshing techniques. Each scheme has its own strengths and weakness and recent studies clearly show a diversity of method applied with no significant dominance of any one numerical scheme. Furthermore, in spite of the improvement of computational resources, there are still doubts over the accuracy of CFD based methods due to the sensitivity of the solution to grid spacing and time step size. For a three-dimensional full-scale ship calculation CFD methods still require very large computational effort, which limits their application as a practical ship design tool.

Many computational results for ship motions using CFD methods were produced in the last few years (refer to Table 6 for an overview of CFD methods used for seakeeping). Orihara and Miyata (2003) solved the ship motions problem in regular head wave conditions and evaluated the added resistance of a series of different bow-form for a medium-speed tanker in regular head waves using a CFD simulation method called WISDAM-X. The Reynolds-averaged Navier-Stokes (RANS) equations were solved by the finite-volume method with an overlapping grid system.

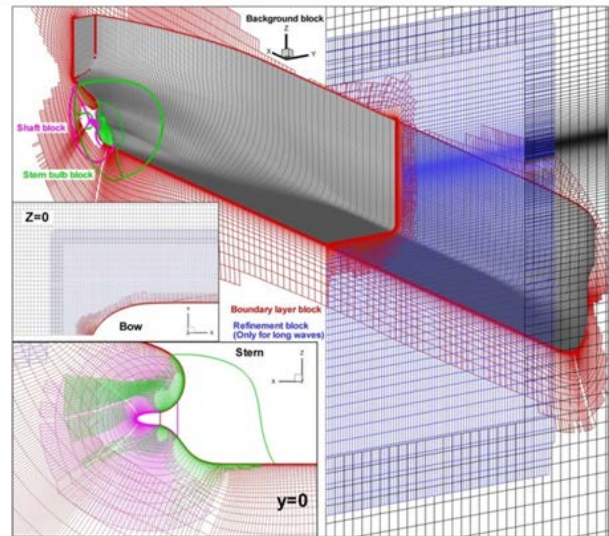


Figure 27. Overset grid system (Sadat-Hosseini et al., 2013)

The group at Iowa University has led many research projects on the ship resistance problem using CFD methods. Based on their past experience in CFD computations, their work has extended to manoeuvring and seakeeping problems in recent years. For example, Carrica et al. (2007) solved RANS equation with single-phase level set method for surface ships free to heave and pitch in regular head waves. The overset grid system which is shown in the Figure 27 was used for a rigid body movement. More recently, Sadat-Hosseini et al. (2013) validated CFD Ship-Iowa V4.5 for the ship motions and added resistance of KVLCC2 tanker advancing at $Fn=0.142$ with fixed and free surge in head waves.

Dommermuth et al. (2007) simulated breaking waves around ships and prescribed the motion problem by Numerical Flow Analysis (NFA) code based on a combination of Cartesian-grid methods and volume-of-fluid methods. A ship hull was represented on a Cartesian grid by an immersed boundary generated from the panelled ship hull surface data. They used a Smagorinsky turbulence model, which is an LES scheme for computation of turbulence phenomena in the flow field, while a free slip

boundary condition was adopted for the body boundary condition and an empirical model for shear stress was used for friction of body.

Hu and Kashiwagi (2007) developed a CFD-code named Research Institute for Applied Mechanics, Computation Method for Extremely Nonlinear hydrodynamics (RIAM-CMEN) which adopted a constrained interpolation profile (CIP) based Cartesian grid method. In the CIP-based formulation, the wave-body interaction problem is considered as a multi-phase problem. Different phases are recognized by a density function that has a definition similar to the volume fraction function in the VOF method. To calculate the volume fraction of the solid phase, virtual particles were used. They compared the THINC scheme and the CIP scheme as an interface capturing method and showed the possibility that a CIP-based method could be applied to simulate strongly nonlinear wave-body interaction problems for modified Wigley models. Hu et al. (2008) conducted computation for green water effects in large amplitude ship motion of S-175 containership as shown in Figure 28.

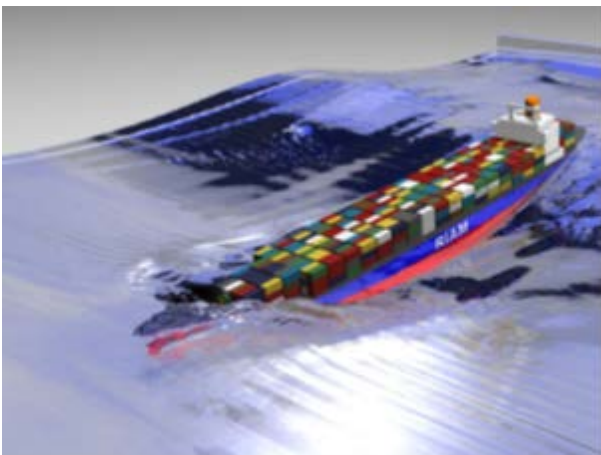


Figure 28. S-175 containership advancing in large amplitude head waves (Hu et al., 2008)

Visonneau et al. (2010) conducted analysis for ship motion problems using their CFD pro-

gram called ISISCFD. This program used improved gamma differencing scheme for discretization of the convection term, and the RANS solver was applied to computation of the turbulence effect. One of the main characteristics of this program is using an unstructured hexahedral grid and an analytical weighting mesh deformation approach for a moving body. This program was also validated by Guo et al. (2012) for calculating the added resistance of KVLCC2 in head waves.

Monroy et al. (2009) validated a spectral wave explicit Navier-Stokes equation (SWENSE) method to solve the ship motion problem in irregular head waves. In the SWENSE method, incident wave terms are calculated by a potential flow model and diffracted wave fields are solved based on the RANSE equation under a structured body-fitted grid system. Due to the potential based theory, this program can have the capability for simulating ship motions in irregular waves. They carried out computation for heave and pitch motion in irregular waves using this approach.

Yang et al. (2013) simulated large-amplitude ship motions by using a finite-volume based method on a non-uniform Cartesian grid. Viscous effects were ignored and the wave-body interaction problem was considered as multi-phase problem with water, air, and solid. The volume fraction of a solid body embedded in a Cartesian grid system was calculated by a level-set based algorithm and systematic numerical simulations for Wigley III hull and S-175 containership in regular head waves were conducted.

Particle methods have also been applied to wave-body interaction problems. Sueyoshi (2004) and Doring et al. (2004) conducted computations for motion analysis of two dimensional floating bodies with a hole using a particle based method such as moving particle



semi-implicit (MPS) and smoothed particle hydrodynamics (SPH). These efforts may be a useful foundation for damaged ship analysis.

Figure 29 shows some sample results of the pierced box case.

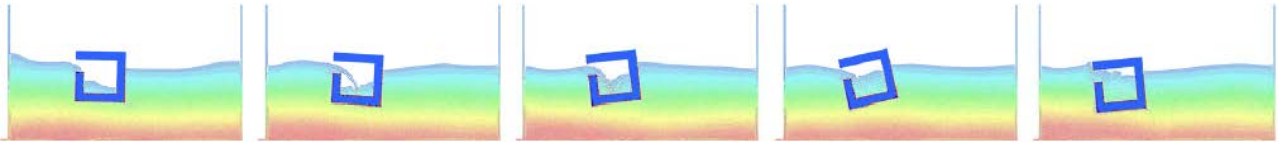


Figure 29. Pierced box test case (Doring, 2004)

As well as the above applications of proprietary codes, there have also been applications of open source and commercial CFD software to wave-body interaction problems. Moctar et al. (2010) calculated the ship motions in regular head waves for $\lambda/L=0.6$, 1.1, and 1.6 by using Comet and OpenFOAM based on the RANS equations with finite-volume approach. Test ships were a containership (KCS) and an oil tanker (KVLCC2). Recently, the same group has continued to simulate violent ship motion by using OpenFOAM and STAR-CCM+. The commercial software Star-CCM+ developed by CD-adapco is becoming popular and Kim et al. (2013) showed the CFD simulations of ringing response of a gravity based structure in extreme sea states using this technique.

A comparative study for various seakeeping tools was conducted by Bunnik et al. (2010). A container ship and a ferry were chosen for model ship. For the container ship, rigid body motions including hydrodynamic coefficients, added resistance, internal loads and relative vertical motions all calculated for 24.5 knots in head seas while for the ferry, rigid body motions, internal loads and relative vertical motions were compared for 25.0 knots in head seas. All the numerical results were compared with experimental data. In this comparative study, the participants based on CFD methods were as follows:

- ECN-CFD : CFD based method using RANS solver, “ISISCFD” (Ecole Centrale de Nantes)
- GL-CFD : CFD based method using unstructured FVM RANS solver, “COMET” (Germanischer Lloyd)
- KU-OU-CFD : CFD based method using CIP and THINC scheme, “RIAM-CMEN” (Kyushu University and Osaka University)

For these test models, there was no clear advantage of any particular CFD based method compared with potential flow based methods, as long as there are no strong nonlinearities or viscous effects. Also, numerical codes using nominally the same method can produce different results meaning that the choice of numerical scheme and the procedure of implementation are both of critical importance for seakeeping problems.

Another comparative study of CFD methods for seakeeping was conducted by Larsson et al. (2010). In this comparative study, the performance of various CFD based methods was compared. Although most test cases were for steady wave problems such as prediction of ship resistance, in some cases, the ship motions, added resistance and roll decay were compared with experimental data. Test cases were for the KVLCC2, KCS and DTMB 5415.



Larsson et al. (2011) analyzed the results of the comparative study and pointed out that the number of grid points has an obvious effect on both motions and resistance results. The prediction error is around 16 %D (standard deviation) for 1st harmonic motion amplitude and the smallest error averaged over amplitudes and phase for motions is 2.66%D for CFDShip-Iowa with the largest number of grids, 4.73M grid points. A comprehensive analysis of all results is published in Larsson et al. (2014).

A detailed study of both steady and unsteady ship motions is considered in Simonsen et al. (2013), who compare experimental results for the KCS to CFD predictions using both Star CCM+ and CFDSHIP-IOWA and a potential flow method. Attention is paid to the uncertainty of both the measured and predicted quantities. Overall agreement of the CFD with the experimental data is good, with the steady-flow quantities better predicted than the unsteady motions. In waves, the mean resistance was accurately predicted by the CFD, but the amplitude of the resistance variation with time is underpredicted. This is consistent with other studies of the same phenomena using CFD.

A further comparison of the accuracy of CFD methods to predict added resistance in waves is found in Soding et al (2012) where a comparison to a potential flow Rankine Panel Method and experiments is made for a container ship advancing in head waves. Predictions from the CFD method are close to experimental results in the long wave region, but less accurate in shorter waves.

An example of the application of an overlapping grid method applied to large amplitude motions predicted using the Star CCM+ code is found in Peric and Schreck (2012), where cases of a free-fall lifeboat entering the free surface and the KRISO container ship advancing in oblique waves are addressed.

Although CFD based methods can be applied to wave-body interaction problems, they generally require massive computational time and thus offer few advantages unless violent flows or highly nonlinearity are involved. Thus, many studies have focused on CFD computation to simulate violent local flows rather than three-dimensional wave-body interaction problems. Sueyoshi et al. (2005) have applied the MPS method for sloshing problem of a two dimensional tank. Nam and Kim (2006) introduced the application of SPH, and Kishiev et al. (2006) have applied a CIP scheme for violent sloshing problems. Level-Set and SPH methods have been applied by Colicchio (2007) for flip-through phenomena during sloshing flows and compared with experimental results. Kim (2007) described experimental and numerical issues in sloshing analysis, and the comparison between the SPH and SURF schemes has been introduced. Wemmenhove et al. (2009) solved three-dimensional violent sloshing problems by using ComFLOW code. Typical results of fluid configuration are shown in Figure 30.

For the slamming problem, CFD methods are not generally useful because the impact pressure is quite sensitive to grid resolution and time step. The water entry problem with impact occurrence is strongly nonlinear and regarded as a non-memory problem, where the impulsive pressure variation is involved in a similar manner to sloshing-induced impact. This problem has been tackled by using SPH. Good examples can be found in the work of Oger et al. (2006, 2007) which solved 2D and 3D water entry impact problems. Kim et al. (2007) also applied the SPH method for the water entry of wedges, and free surface evolutions have been compared with experimental results. Particularly, SPH has been applied for simulating both the non-cavity and cavity flows during impact. Recently, Oger et al. (2009) extended their SPH method to simulate hydroelastic impacts

with strong fluid-structure coupling. An example of their results is shown in Figure 31.

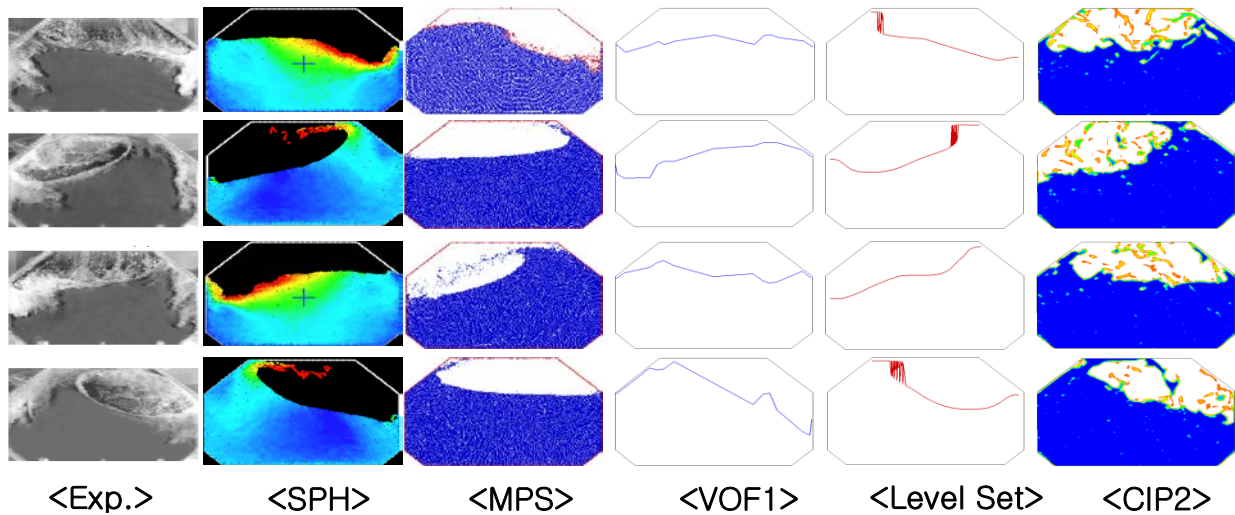


Figure 30. Comparative study of sloshing simulation (ISOPE, 2009)

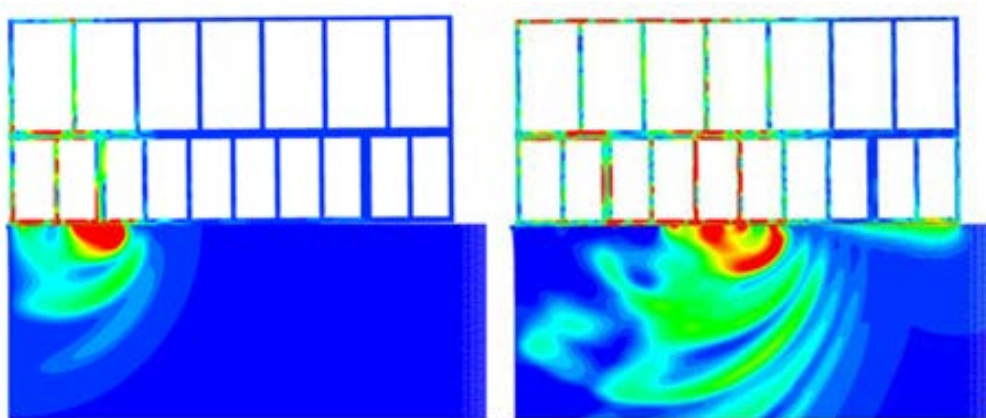


Figure 31. Visualisation of pressure field in water and Von Mises equivalent stress in structure at various instants, Oger et al. (2009)

5. OVERVIEW OF SLOSHING EXPERIMENTS

5.1. Introduction

Liquefied natural gas carriers (LNGCs) with capacities of 138,000–145,000 m³ were the most popular in the market from the 1970s to the 1990s. Starting in 2000, though, construction of larger LNGCs increased dramati-

cally, and LNGCs with capacities greater than 180,000 m³ appeared in the late 2000s (Figure 32). Although the capacity of LNG carriers has been increased dramatically, the size of the loads has remained nearly unchanged. Such unbalance can result in the significant increase in sloshing loads in liquefied gas tanks.

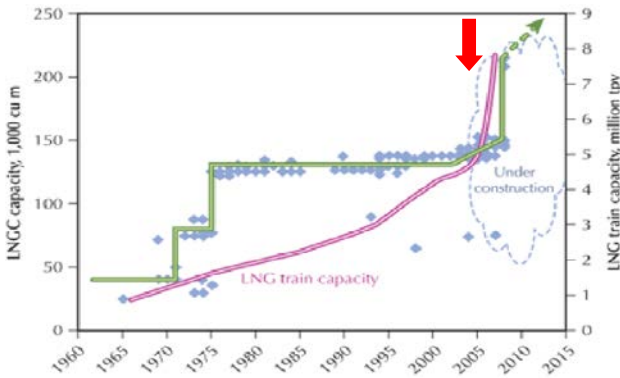
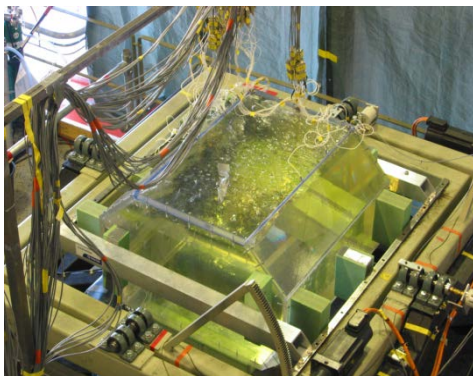


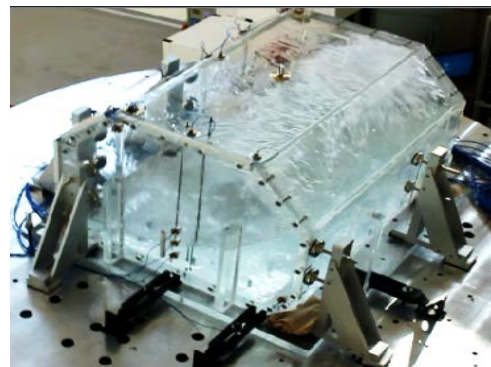
Figure 32. Recent trend of LNGC capacity

The two major concerns in sloshing problems are the prediction of impact loads and coupling with floating-body motion. The latter concern is related to the motion dynamics of ships or offshore structures, but the former is the main interest in LNG carrier design. Despite many previous theoretical and computational efforts to predict sloshing pressure, model scale testing is still considered as the most reliable approach for practical purposes. Analytic approaches cannot simulate violent

sloshing flows with strong nonlinear phenomena, and computational fluid dynamics (CFD)-based computation is not yet an appropriate tool to replace experimental methods. For this reason, in the last decade, highly systematic methodologies or concepts for the experimental assessment of sloshing loads have been studied (e.g., Graczyk et al., 2006; Kuo et al., 2010), and a few large experimental facilities have been built for practical model tests. Such large facilities with capacities of more than 3- or 4-tonne payloads were installed at GazTransport and Technigaz (GTT), Marintek, Pusan National University, and Seoul National University (SNU) (Figure 33). In particular, very recently, a hexapod with a payload of more than 10 t was introduced by SNU. This trend is mostly due to the demand for larger-scale model tests, which implies that the importance of and interest in sloshing are increasing among not only naval architects but also ocean engineers.



(a) Marintek



(b) SNU

Figure 33. Practical model-scale sloshing experiment (Marintek and SNU)

Many studies were conducted in the 1970s and 1980s, which were mostly limited to small scale-model tests and/or 2D experiments, to understand the physics of sloshing phenomena and determine the magnitude of sloshing-induced impact pressure on LNG containment systems. Based on this foundation, larger-scale

and 3D experiments have become more popular since the late 1990s and 2000s. Nowadays, the typical model scale of sloshing experiments for practical LNG carrier design is in the range of 1/60–1/40, and the 1/50 scale has become a sort of standard size for model tanks.



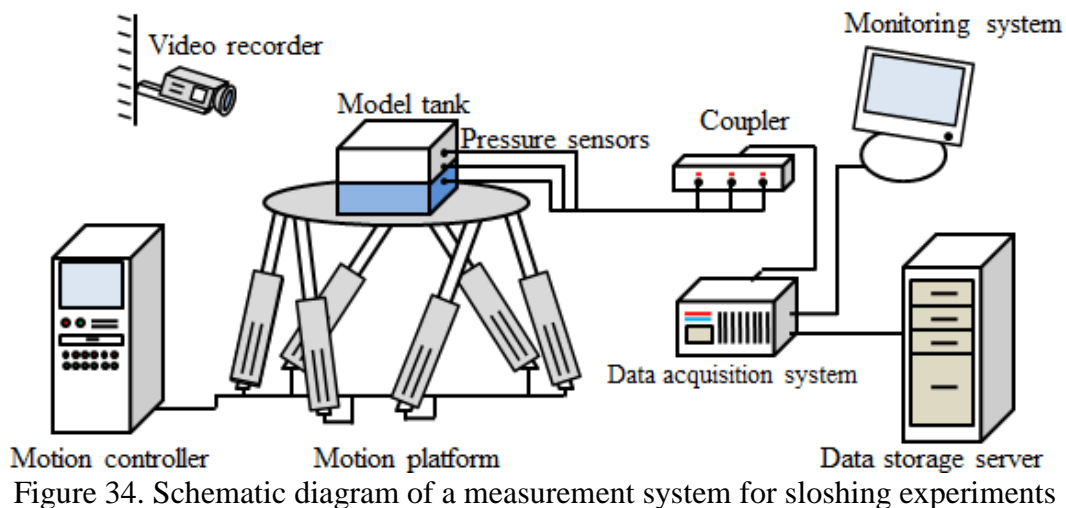
Recently, high-performance data acquisition and large data storage systems have allowed the capture of sloshing impact simulations with a high sampling rate. Many studies have been conducted based on an experimental approach (Lugni et al., 2006; He et al., 2009; Maillard and Brosset, 2009; Yung et al., 2009). A real-scale impact test was carried out at the Maritime Research Institute Netherlands (MARIN) (Brosset et al., 2009; Kaminski and Bogaert, 2009). Previous experimental studies were focused on sloshing phenomena and investigation of the scale effect on sloshing. Many research activities were highlighted in the Sloshing Dynamics Symposium of the International Society of Offshore and Polar Engineers (ISOPE) conference. Very recently, an ISOPE sloshing benchmark test was carried out (Loysel et al., 2012), and the differences between the experimental results of various experimental facilities were observed.

In spite of the considerable efforts expended in experimental analysis, there are many uncertainties in these sloshing experiments. Recently, Souto-Ilesias et al. (2011) discussed uncertainty analysis of the experimental setup. In terms of experimental instruments, Choi et al. (2010) tested two piezoelectric sensors and discussed the effects of thermal shock, sensing diameter, and improper mounting on the sloshing pressure. Pistani and Thiagarajan (2012) thoroughly examined a motion platform, a pressure sensor, and a data acquisition system and observed the characteristics of instruments. Except for those papers, it is difficult to find studies on errors analysis of experimental instruments.

In sloshing experiments, in addition to uncertainty, there are many technical barriers to the accurate measurement of impact pressure, e.g., the sensitivity of pressure sensors, scale effects, and appropriate media to simulate LNG-NG flows. Because there is no experimental technique on which everyone agrees organizations with large sloshing experimental facilities and classification societies have their own procedures for sloshing experiments. Some procedures or techniques are common, but there are some differences in the detailed methodology. However, it should be mentioned that while some procedures/techniques are common, it does not mean that they are the best or most appropriate. That is, there are still many uncertainties in sloshing experiments, which are not clear or validated. Therefore, it is not appropriate to develop or suggest a unified procedure for sloshing experiments at this time. Instead, the committee would like to summarize the current status of model-scale sloshing experiments and the guidance/recommendations of classification societies.

5.2. Sloshing Experiment: Overview

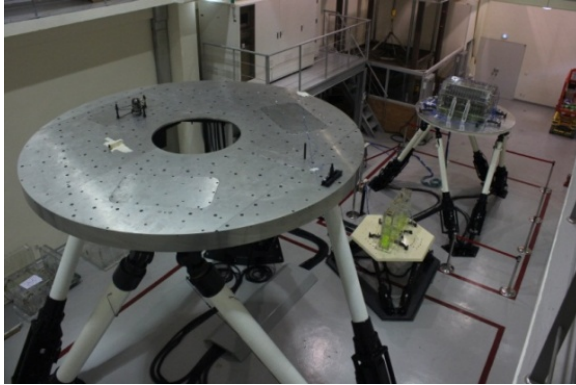
Figure 34 shows a typical schematic diagram of a measurement system for sloshing experiments. A motion platform, which is controlled by a motion controller, provides a model tank with six degrees of motion. Then, pressure sensors installed in the tank measure the dynamic pressure on the tank walls. A data acquisition system converts electric pressure signals into digital data. The acquired data is monitored in real time and saved to a data storage server.



5.2.1. Motion Platform

In the model-scale sloshing experiment, a motion excitation bed is essential to simulate the motion of the tank (i.e., motion of a ship or offshore structure). There are a few types of excitation bed. In the case of MARINTEK (Figure 33), a moving table with rotating axes is used to simulate motion. However, the most typical type is the hexapod-type platform shown in Figure 35. A hexapod platform comprises six actuators that can move vertically and transversely. Linear actuators are typically equipped to minimize the time lag between the controller and the actuators.

There are about 10 facilities with hexapod platforms with payload capacities of 1~2 tonne. Such small platforms can be used for 1/100–1/60-scale tests for 3D model tanks and up to 1/50-scale tests for 2D models of typical LNG carriers or LNG floating production storage and off-loading (FPSO) facilities. For practical experiments, i.e., for predicting sloshing loads or the certifying classification societies, a 1/50–1/40 scale experiment should be carried out. In this case, a hexapod platform for a payload simulation of 2–6 tonne is needed. At present, only a few facilities have this capacity. In the case of GTT, a platform with a 6-ton capacity is being used. Very recently, SNU installed three motion platforms with payload capacities of 1.5, 5, and 14 tonne that can conduct experiments of up to 1/20 scale with a 3D model tank.



(a) SNU (3 platforms of different sizes)

(b) GTT

(c) PNU

Figure 35. Hexapod platforms for sloshing experiments (over 4-tonne dynamic payloads)

The greatest technical difficulty in the design and fabrication of a large platform is the severe requirements of the motion characteristics. Since violent sloshing flows typically occur in harsh environments, all the motion properties, i.e., displacement, velocity, and acceleration, must be large enough to simulate the severe motion responses of ships and offshore structures. Furthermore, the accuracy of motion signals should be carefully checked. The accuracy of motion displacement and phase shift can be observed by using motion sensors such as optical sensing devices, accelerometers, and/or potentiometers. To this end, it is desirable to use multiple sensing devices to cross-check accuracy. If the error in the motion amplitude is larger than 3%–5%, the platform motion sensors should be calibrated to increase their accuracy.

5.2.2. Model Tank

A model tank is generally made of acrylic so that the detailed flow can be visually observed. Figure 36 shows typical 2D and 3D models for sloshing experiments. The model tank should be water-tight and the wall surface should be very flat and smooth if there is no particular reason to make it rough, so that sloshing flow

is not affected by surface roughness. It is also important for the thickness of the acrylic layer to be sufficient to minimize the hydroelastic behavior of a model tank. When the wall thickness is not sufficient, the sloshing impact loads can cause hydroelastic vibration of a model tank, consequently resulting in unreliable measurement of pressure and flow.

Before an experiment with partial filling, it is desirable to carry out a hammering test. The results of the hammering test can be used to predict the natural frequency of tank wall vibration, and the period of this natural mode should be much smaller than the typical duration of sloshing-induced impact pressure, so that the effect of hydroelastic vibration will not have any effect on the impact process.

When heavy gas is used in sloshing experiments in order to match the density ratio between LNG and NG, rather than that between water and air, the model tank should be gas proof. It is very important to ensure that the heavy gas does not leak during the experiment. Heavy gas (SF_6 is typically used) can be harmful to humans, so safety should be guaranteed during the experiment.

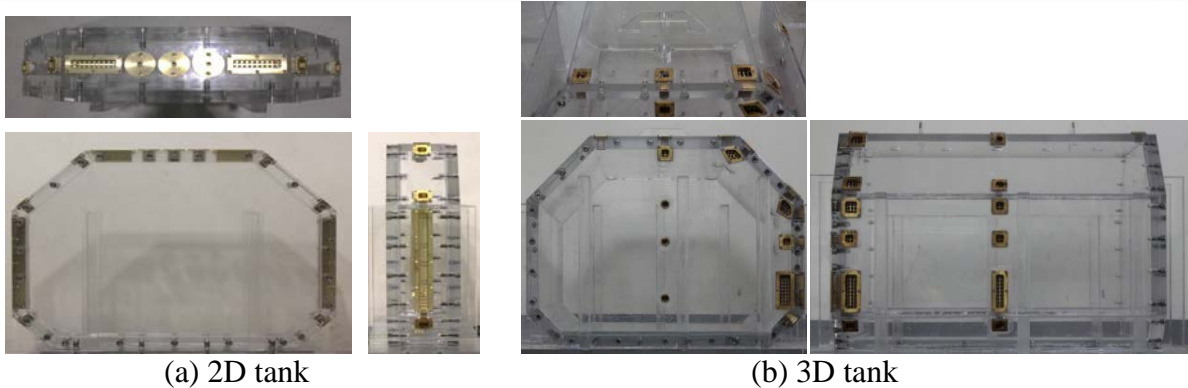


Figure 36. 2D and 3D model tanks

5.2.3. Pressure Sensor

Pressure sensors can be the most important of all experimental instruments. The motion platform can be calibrated by measuring the displacement of the input and output. The error of a data acquisition system is relatively lower than that of other instruments. A model tank can be the source of error, but that error can be minimized by the manufacturer. However, the error from the pressure sensors in the sloshing experiment has yet to be accurately estimated. Linearity, hysteresis, and resolution of a pressure sensor can be evaluated, and calibration can be performed using a reference sensor or an impact test in air. However, those cannot guarantee the accuracy of sloshing pressure, because sloshing impact occurs within a very short time, and the medium contacting the sensor suddenly changes from gas to liquid. The pressure sensors are typically not calibrated in that situation.

There are various types of pressure-sensing technologies, such as piezoresistive, capacitive, electromagnetic, piezoelectric, optical, and potentiometric. For measurement of sloshing load, piezoelectric sensors are mainly applied, and pressure sensors from the three manufacturers Kistler, Kulite, and PCB are popular as shown in Table 7. The sensors by Kulite are mainly piezoresistive (Kulite, 2004), while those of Kistler and PCB are mainly piezoelec-

tric. Many pressure sensors used in previous studies have small sensing diameters of about 2.5–5.5 mm. The pressure sensor should be small as possible and have a high natural frequency because large sloshing impacts occur in a very small region within a very short time. Moreover, the pressure sensor needs to be capable of measuring in two-phase flows over a large pressure range.

Piezoresistive sensors are not affected by temperature differences between the sensor and the medium. Furthermore, they are effective in measuring slowly varying pressure. However, piezoelectric sensors are regarded as a mature technology with outstanding inherent reliability. Piezoelectric materials typically have a high modulus of elasticity and thus nearly zero deflection and extremely high natural frequencies. Moreover, they have excellent linearity over a wide amplitude range. Therefore, piezoelectric sensors are appropriate for sloshing experiments. However, it is known that an additional signal can be generated when the sensor contacts a medium with a different temperature. This can be a problem when measuring sloshing pressure because there can be a temperature difference between the gas and the liquid. Therefore, this sensor is not effective for measuring static pressure, which produces a constant loss of electrons, resulting in signal drift.



Piezoelectric sensors for sloshing experiments can be categorized into two types. The first is charge-mode-type sensors, which require an amplifier to measure pressure signals. The second is integrated electronics piezoelectric (IEPE) or integrated circuit piezoelectric (ICP) sensors, which have an amplifier built into the sensor. The charge-mode-type sensor is good for high temperatures, and the sensitivity of the sensor can be changed. However, they take up a huge amount of space when a large number of measuring points are required. ICP

sensors have fixed sensitivity, but the measuring system is relatively simple. Therefore, ICP sensors are mainly used in many sloshing facilities. In sloshing experiments, it has not yet been determined which type of pressure sensor is best to be used for measuring the sloshing impact pressure. The piezoelectric sensor is regarded as being better than the piezoresistive sensor for capturing impact pressure changes that occur within 1~10 ms.

Table 7. Main features of pressure sensors for sloshing experiments

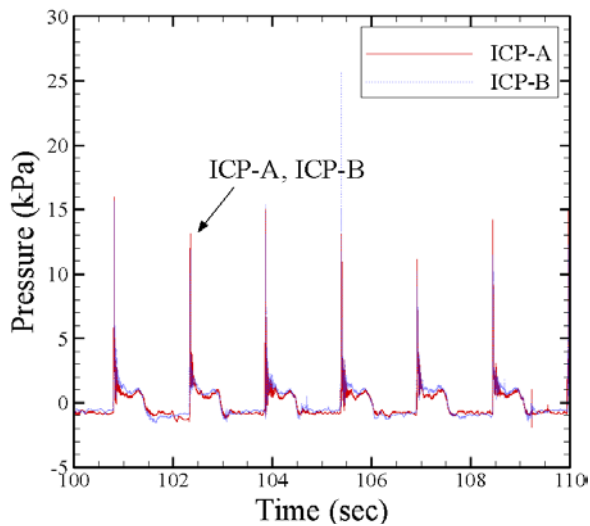
Group	Maker	Model	Diameter (mm)	Reference
Ecole Centrale Marseille	PCB	112A21	5.5	Loysel et al. (2012)
Exxon Mobile	Kulite	XCL-8M-100-3.5BARA	2.6	Yung et al. (2009)
GTT	PCB	112A21	5.5	Loysel et al. (2012)
MARINTEK	Kulite		~2.5	Loysel et al. (2012)
Pusan National Univ.	Kistler	211B5	5.5	Choi et al. (2010)
Seoul National Univ.	Kistler	211B5	5.5	Kim et al. (2011)
Technical Univ. of Madrid	Kulite	XTL-190	~2.5	Souto-Iglesias et al. (2012)
Univ. of Duisburg-Essen	Kulite	XTM-190	3.8	Loysel et al. (2012)
Univ. of Rostock	PCB	M106B	11	Mehl and Schreier (2011)
Univ. of Western Australia	Kulite	XCL-8M-100-3.5BARA	2.6	Pistani and Thiagarajan (2012)

Recently, Ahn et al. (2013) conducted a comparative study on several pressure sensors in sloshing experiments. They used one piezoresistive sensor and three piezoelectric sensors, including two ICP sensors, in 2D tank tests, and tested and compared the sensitivity to temperature differences between the sensors and the medium by exposing the sensors to hot

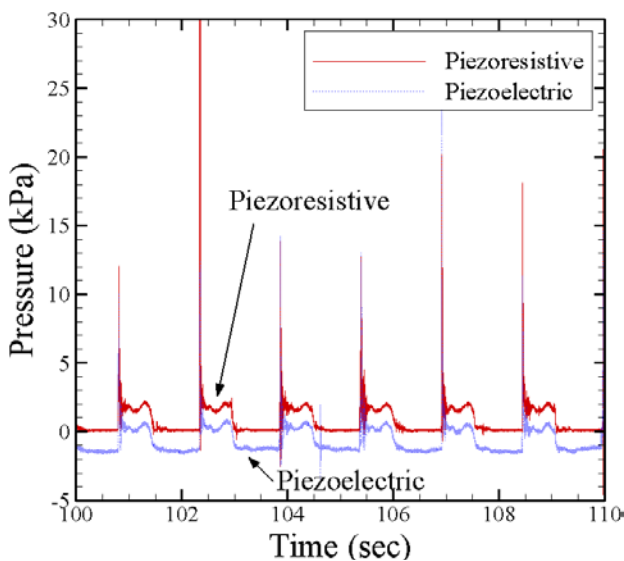
and cold water. Sloshing pressures during the regular and irregular motions were also measured. Figure 37 shows an example of results from their comparative study.

Pressure measurement can be performed by using not only a single pressure sensor but also a cluster of sensors. Pressure sensors in 2×2 , 3

$\times 3$, 4×4 , or any other $n \times m$ combination can be installed to measure local pressure in a certain area. Figure 38 shows two clusters sensors with 3×3 and 2×2 configurations. These can be used to analyze the spatial distribution of pressure and observe the averaged local pressure or force in the measured area.

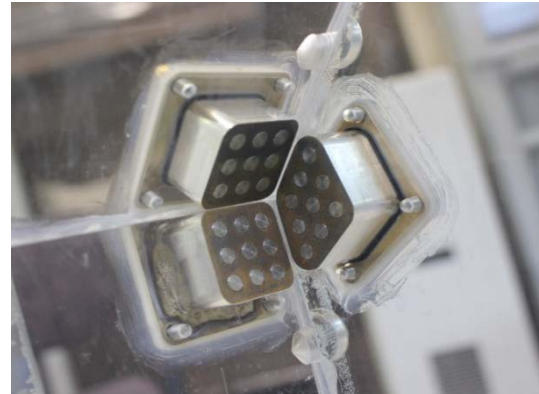


(a) Piezoresistive and piezoelectric sensors

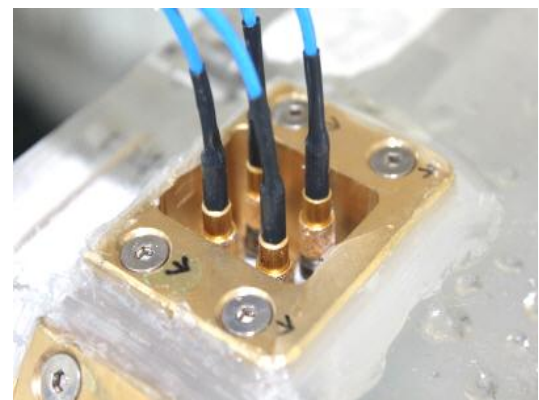


(b) ICP sensors

Figure 37. Time histories of pressure signals measured in a 2D tank under surge motion with 20% H filling (Ahn et al., 2013)



(a) Metal adaptors for a 3×3 cluster around a corner



(b) Installed 2×2 cluster of sensors
Figure 38. Examples of cluster sensors

The following tests are recommended before the selection of pressure sensors for sloshing tests:

- Slowly varying pressure test
- Test of sensitivity to temperature differences between liquid and sensor
- Test of sensitivity to the test medium, e.g., water or other liquid
- Drift test for long measurement time
- Motor noise test

Metal adaptors are commonly employed to increase the reliability of pressure measurement by pressure sensors. Bronze is the typical material for adaptors. This type of adaptor can give more reliable and stable pressure signals. Furthermore, it is very important to maintain the



same temperature in the sensor and fluid. This can be achieved by exciting fluid motion for a certain time and allowing the temperatures of the contacted fluid and sensor surfaces to equalize.

5.2.4. Sampling Rate and Time Window

It is known that the sampling rate in sloshing experiments should be high in order to capture spikes in sloshing pressure. In general, it is agreed that 20 kHz or greater is acceptable for most sloshing experiments (Kim et al., 2012; Maillard et al., 2009; Ryu et al., 2009).

The size of the experimental time window is still under discussion. Since impact pressures occur randomly and the magnitudes of peak pressures are also random, the size of the time window can be a critical parameter in the statistical analysis of impact loads. Thus far, a 5-h time window in real scale has been popular for irregular experiments, but recent studies have shown that this may be insufficient for practical LNG cargo containment system (CCS) design (e.g., Ahn et al., 2013). It is not yet clear what the optimum time window should be, but a minimum measurement time of 50 h has been recommended by SNU and a measurement time of 200 h been suggested by Bureau Veritas.

5.2.5. Test Conditions

For the prediction of design loads due to sloshing, the selection of the appropriate ocean (i.e., motion) condition is a critical element in sloshing experiments. It is strongly recommended to carry out prescreening tests to determine irregular wave conditions. However, in practice, such prescreening tests incur a large cost and require a long time. Therefore, the type and number of the prescreening tests should be carefully chosen. For the ocean conditions to be used for main experiments, re-

peated tests are strongly recommended. These repeated tests with different phases of wave components, i.e., motion components, are desirable to reduce the error or uncertainty of random signals.

When a prescreening test cannot be conducted owing to cost and/or time limitations, a typical set of conditions for sloshing experiments is listed in Table 8.

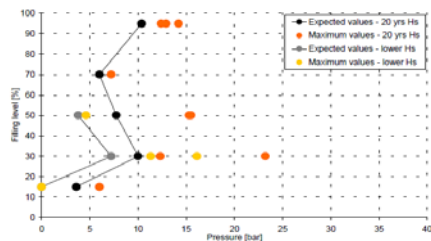
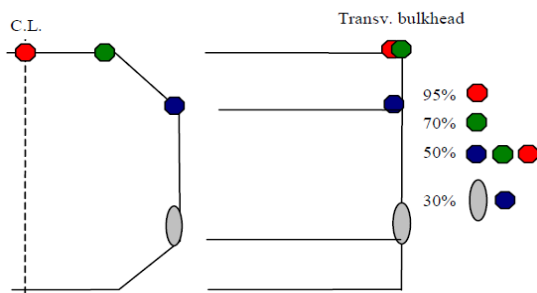
Table 8. Typical experimental conditions for irregular motion (real scale)

Test condition	Description
Filling levels	15%, 30%, 70%, and 95% of tank height
Ship speed	5 knots
Heading angles	150° and 90°
Sea states	T_z (modal period): 9.0 s and 11.0 s H_s (significant wave height) of 40-year return period for a 150° heading, and 1-year return period for a 90° heading
Measurement time	5 hours for each case
Test repetitions	At least 2 times

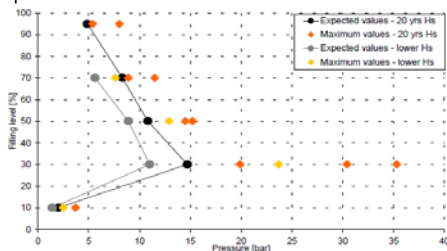
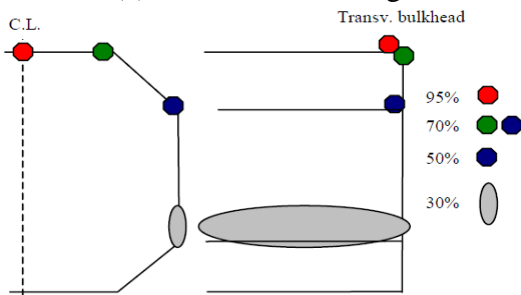
5.2.6. Measurement Area

It is obvious that sloshing pressure varies in space. Therefore, the pressure sensors should be installed in areas where largest impacts occur. In general, large sloshing pressures are measured around the still-water level in low filling conditions and around the upper chamber or the tank top in high filling conditions (see Figures 39 and 40). Therefore, more sensors should be installed in these areas.

In a practical experiment, e.g., for the design of an LNG CCS, more sensors are better in order to cover more areas. In particular, for areas of high impact pressure, the installation of cluster sensors is highly desirable. It is also important to understand that the magnitudes of impact pressures can differ between the weather and lee sides; therefore, the locations of the sensors should be carefully chosen.



(a) 180° wave heading



(b) 90° wave heading

Figure 39. Sloshing impact areas (Pastoor et al., 2004)

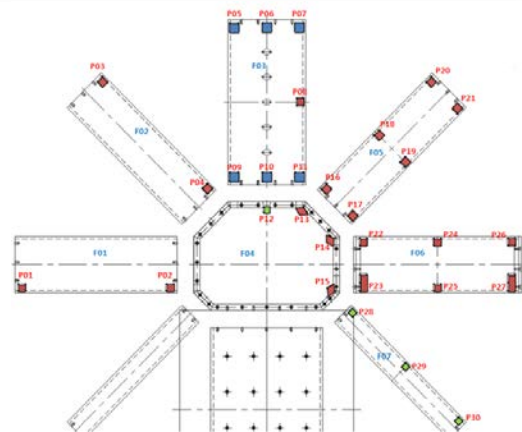


Figure 40. Example of sensor locations for a 3D model

5.3. Statistical Analysis of Sloshing Impact Pressure

5.3.1. Peak Sampling

In statistical analysis, peak pressure signals need to be sampled for the entire pressure time history. Sampled sloshing peaks, or global peaks, are chosen by imposing a set of threshold pressure and sampling time windows (Figure 41).

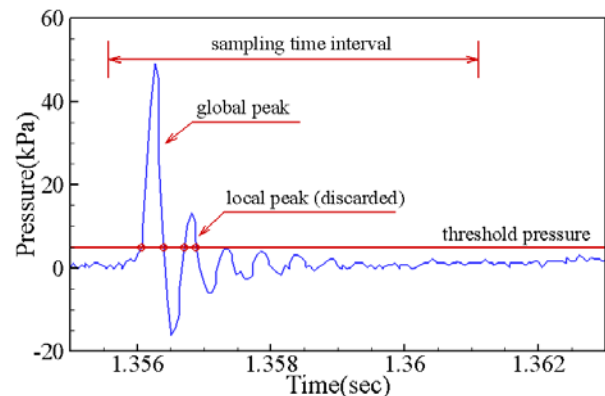


Figure 41. Methodology of peak sampling

Within a moving time window, the largest peak signal is sampled as the global peak, and others are disregarded in the analysis. The maximum pressures collected from all the

segments become a set of sampled peaks for statistical analysis. Therefore, the set of sampled data is dependent on the threshold pressure and the sampling time interval. The threshold pressure plays a key role in this selection process. However, the criteria for selecting these parameters have yet to be clearly defined. Therefore, the moving window size and the threshold are varied to determine the reliability of the results.

5.3.2. Peak Modeling

Sampled peak pressure signals can be modeled as simple triangular shapes, and thus, the characteristics of the peaks can be determined. Figure 42 shows an example of peak modeling and the main characteristics of a peak: peak pressure (P_{max}), rise time (T_{rise}), decay time (T_{decay}), and total time (T_{total}). Peak pressure is defined as the maximum pressure value of the peak. However, definitions of rise time and decay time are different in many studies. According to existing studies and guidance notes from classification societies, rise time and decay time can be categorized as follows:

- Type 1: Absolute thresholding:

$$T_{rise} = t_{P_{max}} - t_{P_{threshold\ up-crossing}}, \quad (19)$$

$$T_{decay} = t_{P_{threshold\ down-crossing}} - t_{P_{max}}. \quad (20)$$

- Type 2: Relative thresholding:

$$T_{rise} = \frac{t_{P_{max}} - t_{(\alpha_{rise} \cdot P_{max})\ up-crossing}}{1 - \alpha_{rise}}, \quad (21)$$

$$T_{decay} = \frac{t_{(\alpha_{decay} \cdot P_{max})\ down-crossing} - t_{P_{max}}}{1 - \alpha_{decay}}. \quad (22)$$

where $t_{P_{max}}$ is the time when the peak pressure P_{max} occurs; the subscript indicates the time when pressure becomes $\alpha_{rise} P_{max}$, $\alpha_{decay} P_{max}$. The up-crossing time is considered for the rise time and the down-crossing time is considered for the decay time. Type 1 thresholding applies the time when a certain absolute pressure is found, regardless of the peak value. Conversely, type 2 thresholding measures the rise and decay times at the instants when the pressure crosses the up and down percentages ($100 \times \alpha$) of the peak pressure, respectively. This method, based on a relative-pressure concept, defines the times at which the rise and decay times should be measured. Table 9 presents the current modeling method used by test facilities and classification societies. These different peak modeling methods may predict different impact properties.

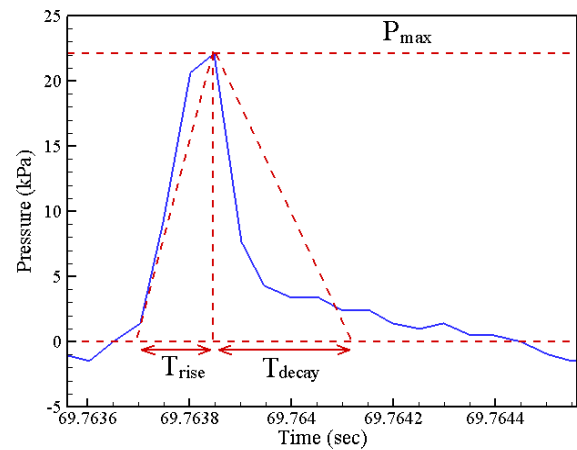


Figure 42. Definition of characteristics of a modeled sloshing peak

Table 9. Current modeling methods used by test facilities and classification societies

	Rise Time	Decay Time
ABS	Type 2 ($\alpha = 0.5$)	Type 2 ($\alpha = 0.5$)
DNV	Type 1 Type 2 ($\alpha = 0.5$)	Type 1 Type 2 ($\alpha = 0.5$)
LR	Type 2 ($\alpha = 0.5$)	Type 2 ($\alpha = 0.5$)
GTT	Type 2 ($\alpha = 0.5$)	Type 2 ($\alpha = 0.5$)
MARINTEK	Type 2 ($\alpha = 0.2$)	Type 2 ($\alpha = 0.3$)

5.3.3. Statistical Distribution

Two methods are popular for statistical analysis for sloshing impact pressures: the three-parameter Weibull distribution and the generalized Pareto distribution. The cumulative probability functions of the two distributions take the following forms:

- Weibull distribution:

$$F(x) = 1 - \exp\left(-\left[\frac{(x - \delta)}{\beta}\right]^\gamma\right) \quad (23)$$

- Generalized Pareto distribution:

$$F(x) = 1 + (1 + cx/\lambda)^{-1/c} \quad (24)$$

In the Weibull distribution function, δ is the location parameter, β is the scale parameter, and γ is the shape parameter. Here, x should be larger than the location parameter. To estimate these three parameters, the method of moments can be applied, which matches the first three model moments—mean, variance, and skewness—with their corresponding sample moments. Figure 43 shows an example of a Weibull distribution fitted on sloshing impact pressure data. In the generalized Pareto distribution function, λ is the scale parameter and c is the shape parameter, both of which can also be estimated by using the method of moments

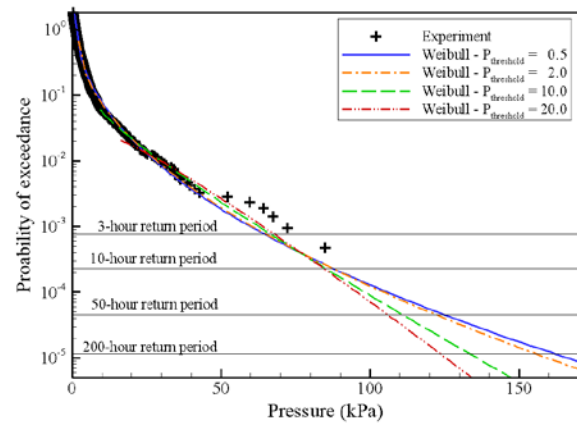


Figure 43. Example of Weibull distribution of sloshing impact pressure

6. COLLABORATION WITH ISSC

6.1. Collaboration with ISSC

The committee has liaised with ISSC, the Ocean Engineering (OE) Committee, and the Specialist Committee on Performance of Ships in Service. Particularly, the committee has been collaborating strongly with the Loads Committee of ISSC. G. Hermanski plays an important role as the liaison of ITTC and ISSC.



6.2. The First Joint ISSC/ITTC International Workshop

The first joint meeting of ITTC and ISSC was held on 8th September, 2012, at Rostock, Germany, with the title of Uncertainty Modelling for Ships and Offshore Structures (UMSOS). (Figure 44) Two ITTC committees, Seakeeping Committee and Ocean Engineering Committee, participated and gave two plenary presentations. Also two ISSC Committees participated in the joint workshop. A panel session followed the plenary presentations and fruitful discussion was made among panellists and participants. A few ideas were proposed to strengthen the collaboration between ITTC and ISSC.



Figure 44. Flyer of 1st ITTC-ISSC Joint Workshop

As a follow-up of this joint workshop, four committees submitted technical papers to Ocean Engineering. Seakeeping Committee

submitted the paper titled “Uncertainties in Seakeeping Analysis and Related Load and Response Procedures”. Y. Kim and G. Harmanski contributed to complete this paper, and the paper was accepted for publication.

6.3. The Second Joint ITTC-ISSC International Workshop

The second joint workshop of ITTC and ISSC will be held in Copenhagen, as a part of ITTC Conference. Like the first joint workshop, the four committees, two of ITTC and two of ISSC, will contribute to the organization and presentation. Lloyd’s Register and Seoul National National University are supporting strongly the joint workshop, and DNV-GL and MARIN are also supporting the organization. (Figure 45)

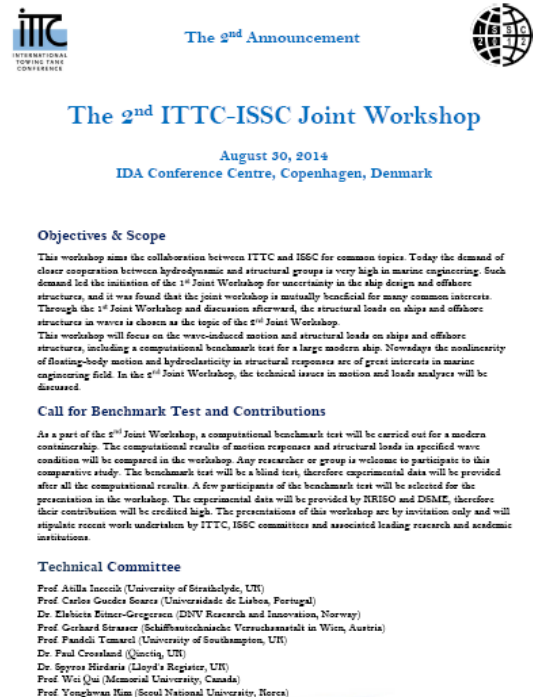


Figure 45. Flyer of 2nd ITTC-ISSC Joint Workshop



In this workshop, a benchmark test for motion and loads on a containership will be carried out. The model ship is a real ship designed and tested in Korea. The benchmark test is a blind test, in which the participants do not know the results of experiment. Several representative results will be presented at the joint workshop.

7. ITTC RECOMMENDED PROCEDURES

7.1. ITTC Procedure 7.5-02-07-02.1, Seakeeping Experiments

This procedure is well written and mature. Therefore, no significant revision was considered. There were proposed changes on sections of the regular and irregular wave sections. It was also proposed that blockage and depth issues should be reviewed. There are several figures without references. Additionally it was considered if there is a better way to look at uncertainty of random processes for the appendix of the procedure.

Based on these suggestions between members, the sections for regular and irregular waves are revised. Also the appendix for uncertainty analysis is revised. The Seakeeping Committee unsuccessfully tried to find the source of Fig.3 - the original document mentions about the 'non published work' of Fernandez. However, the committee members agreed that Fig.3 should be kept since it contains useful information.

7.2. ITTC Procedure 7.5-02-07-02.2, Predicting Power Increase in Irregular Waves from Model Experiments in Regular Waves

It was suggested that the biggest change in procedure should be the inclusion of a section to address directional spectrum with short crested components. It was concluded that other aspects of procedure would essentially remain the same. There was a discussion with regards to applicability of various simulation efforts to calculate added resistance. The thought was whether there would be a future area of the procedure that might incorporate simulation combined with experimental results to determine added resistance. Based on this discussion, some sentences are revised, particularly for the wave spectrum.

7.3. ITTC Procedure 7.5-02-07-02.3, Experiments on Rarely Occurring Events

This procedure was discussed in the general context as to how it should be approached. Ochi's formulae had principally looked at slamming velocity. It was thought that bow flare and hull shape should also be an included factor. In the revision, the definition of slamming has been included.

In the future ABS, ISSC and other classification rules should be reviewed for applicability to slamming and rarely occurring events.

7.4. ITTC Procedure 7.5-02-07-02.5, Verification and Validation of Linear and Weakly Non-Linear Seakeeping Computer

After the review of the procedure and the papers of ITTC Seakeeping Workshop held in Seoul, no changes were recommended by the



committee. However, there was an important comment that the current state of art shows that most authors do not include details of their V&V activities in publications other than straightforward comparison between experimental and computed data, be it RAOs, signal statistics, or direct time trace comparison. This issue should be considered for any future revision.

In the 27th term, the committee could not provide the final draft which includes the description about hydroelasticity computation. The computation procedure for ship structural hydroelasticity can be included in the future or can be a separate procedure.

7.5. ITTC Procedure 7.5-02-07-02.6, Prediction of Global Wave Loads

This procedure was not revised in the 27th term. However the committee discussed combining it with the computational procedure for ship hydroelasticity, but it was recommended not to combine with computational procedure at this stage.

7.6. ITTC Procedure 7.5-02-05-04, HSMV Seakeeping Tests

It was recommended to rewrite data acquisition and data sampling rates. There were only a few paragraphs which need to be addressed, and the references needed to be included.

Some revisions were made as follows:

- References were included (there were none in the previous version)
- A paragraph on placement of 'free to pitch' fitting for catamaran vessels was added
- A requirement to measure pitch inertia was added

- Planing craft testing was updated to include a requirement to consider a appropriate sample rate for human factors measurements
- Free-running model testing was updated to recognise that onboard digital storage is now possible and commonly used. The use of small inertial measurement units for accelerations/motion measurements was recognised
- A minor comment was added on the difficulty of determining the number of wave encounters for planing craft where 'skipping' from wave crest to crest may occur
- The S175 was removed from the suggested benchmark/database of ship. This hull cannot be considered as an HSMV.

8. CONCLUSIONS

8.1. General Technical Conclusions

A few experimental facilities were newly introduced for seakeeping experiment and sloshing. Although numerical schemes are heavily being developed, the importance of seakeeping experiments is still evident through the need to validate numerical codes and to evaluate the seakeeping performance of unconventional ships, e.g. high-speed vehicles and multi-hull ships. The demand to observe very nonlinear phenomena such as nonlinear wave-induced loads, slamming-whipping and green water, is also increasing. Generation of severe ocean environments and investigation of corresponding seakeeping performance is of interest, particularly for offshore structures.

Thanks to the increase of tank size in LNG carriers and offshore structures, the capacity of sloshing experimental facilities is getting bigger. This trend makes it possible to observe larger scaled-model tests than ever. Experi-



tal skills to measure local impact loads have been developed, but there are many technical issues in order to utilise the pressure measured in a model tank for the design of a real-size tank of a ship or offshore structure. At the present stage, it is very desirable to develop an appropriate experimental procedure for model-scale tests and application to ship design. This technical demand is very strong nowadays, particularly for the design of safe LNG cargo tanks of large offshore structures such as FLNG and FSRU.

The Energy efficiency Design Index (EEDI) and Energy Efficiency Operation Index (EEOI) are critical issues for the shipping and shipbuilding industry. The procedures of estimating and verifying CO₂ emission from ships are under intensive discussion at IMO/MEPC and ITTC should cooperate with the IMO. From the viewpoint of seakeeping, the most important parameter is power increase or speed loss in waves. For calculating EEDI, power increase or speed loss in an actual seaway has to be predicted by model tests or theoretical calculations. There is a coefficient f_w in the calculation of EEDI that describes the ratio of ship speed in waves and in wind to that in calm water. A reliable simulation procedure to compute f_w is not yet available..

The most crucial element in the calculation of f_w is to predict added resistance in waves. Besides towing-tank experiments, there are several computational methods, including slender-body theory, 3D panel methods, and CFD application for seakeeping analysis, and direct pressure integration, momentum conservation, and radiated energy methods for added resistance. To date, the most popular method in the shipbuilding field is the combination of slender-body theory and momentum conservation formula, specifically Maruo's formula. However, as computational resources continue to increase 3D panel methods become a strong

candidate to replace slender-body theory and the application of CFD is slowly increasing. For practical ship design, the prediction of added resistance in short waves is crucial. So far empirical formula, such as NMRI's formula seem to be useful up to a certain level, but a practical method to consider nonlinear effects should be developed in the near future.

Ship structural hydroelasticity is an emerging problem in the design of very large ships, such as ultra large containerships. Strip-based approaches combined with a modal approach have been popular in the past, but recent research has focused on the application of 3D panel methods combined with beam approximations. Instead of a beam approximation, a whole ship FE analysis is also considered although it requires significantly larger computational effort. Both towing-tank experiments using segmented models and numerical computation are being used in recent years. Not only for springing but also slamming and resultant whipping are main topics of recent researches.

Seakeeping analysis based on frequency-domain formulation still represents the chosen approach when considering rapid evaluation of prototype designs. However, the popularity of time-domain methods for seakeeping analysis has increased in recent years. This trend is due to the advantages of the time-domain analysis in the extension to nonlinear motion and structural loads, and coupling with external or internal forces. Also the demand for the analysis of ship structural hydroelasticity including slamming and whipping makes the time-domain approach more popular. CFD application is in use in the field of seakeeping, but its robustness and computation efficiency are not yet to a mature state. However, the application of CFD programs, particularly commercial software, is rapidly increasing.



8.2. Recommendation To The Full Conference

Adopt the updated procedure No. 7.5-02-07-02.1 Seakeeping Experiments.

Adopt the updated procedure No. 7.5-02-07-02.2 Prediction of Power Increase in Irregular Waves from Model Tests.

Adopt the updated procedure No. 7.5-02-07-02.3 Experiments on Rarely Occurring Events.

No modification of the procedure No. 7.5-02-07-02.5 Verification and Validation of Linear and Weakly Non-linear Seakeeping Computer Codes.

No revision of the new procedure No. 7.5-02-07-02.6 Global Loads Seakeeping Procedure.

Adopt the updated procedure No. 7.5-02-05-04 HSMV Seakeeping Tests.

8.3. Proposals For Future Work

It is recommended that ITTC has a combination of pure technical committees and special committee(s) for external needs. ITTC has been a technical organization to create and update the procedures for experiments and computation in the marine hydrodynamics field. In the 27th term, the role of ITTC was extended to provide professional comments to IMO and/or ISO and it is desirable that such external need is handled by a special committee(s) which takes charge of non-technical issues. By splitting the committees and their roles, most ITTC committees can remain as pure technical committees.

It is recommended to survey and/or collect benchmark data for seakeeping problems, such

as motions, loads, sloshing, slamming and full-scale measurements. The benchmark data can be very useful to validate the results of experiments and computation. In particular it is recommended to collect the reliable benchmark data of added resistance. The prediction of added resistance is the key element of the prediction of the power increase in waves. To validate and understand the accuracy of computational codes, the reliable benchmark data is necessary.

It is recommended to write a new section for the V&V of ship hydroelasticity codes in the procedure 7.5-02-07-02.5, Verification and Validation of Linear and Weakly Non-linear Seakeeping Computer Codes. If it is too lengthy, it can be a separate procedure. It is recommended that the developed section/procedure is reviewed by the ISSC Loads and Responses Committee.

It is recommended to strengthen the collaboration with ISSC committees, including, Loads and Responses and Environment Committees. ITTC Seakeeping Committee and Ocean Engineering Committee, and ISSC Loads and Responses and Environment Committees can share the information relating to nonlinear motion and structural loads and to understand the impact of projected changes in the sea wave environment and the influence the types of wave spectra have in seakeeping experiments. Where there is such overlap with these committees, then collaboration will be valuable. The collaboration can be achieved by the liaison(s) of the committees, but a new working group can be organized for more systematic and active collaboration between ITTC and ISSC.

It is recommended to liaison with Propulsion and Manoeuvring Committees for seakeeping/motion effects. When the ship motion becomes large, the propulsion and manoeuvring performance can be influenced by



motion effects. Also it is recommended to liaise with the Ship Stability in Waves Committee for nonlinear ship motions and statistical analysis of large roll motions.

It is recommended to organize a special committee for sloshing to create a procedure for sloshing model experiments. Due to the high demand of LNG in the world energy market, the construction of LNG carriers and LNG offshore platforms is increasing rapidly. Sloshing is a critical problem of LNG ships and offshore platforms, and hence the number of sloshing experimental facilities has increased over the last decade. However, the procedure for sloshing experiments is not yet fully established. ITTC should create a general procedure for sloshing experiments, particularly focusing on model-scale tank test.

9. REFERENCES

- American Bureau of Shipping (ABS), 2006, "Strength assessment of membrane-type LNG containment systems under sloshing loads", American Bureau of Shipping (ABS), Guidance Notes.
- Advanced Marine Technology, 2010, "Development of large scale sloshing experiment facilities", AMEC Project Report, Seoul National University, Seoul, Korea.
- Ahn, Y., Kim, J.H., Kim, S.Y., Kim, K.H., Kim, Y., 2012, "Particle Image Velocimetry Measurement on the Oscillating Characteristics of Sloshing-induced Internal Flow Fields", Proceedings Of the 6th Asia-Pacific Workshop on Marine Hydrodynamics, Johor, Malaysia.
- Ahn, Y.J., Kim, K.H., Lee, S.W., Kim, Y., 2013, "Experimental Study on the Effects of Pressure Sensors and Time Window in Violent Sloshing Pressure Measurement", 23rd ISOPE, Alaska, USA.
- Ahn, Y., Kim, S.Y., Kim, K.H., Lee, S.W., Kim, Y., Park, J.J., 2012a, "Study on the Effect of Density Ratio of Liquid and Gas in Sloshing Experiment", 22nd ISOPE, Rhodes, Greece.
- Alaoui, A.E.M., Nême, A., Tassin, A., Jacques, N., 2012, "Experimental study of coefficients during vertical water entry of axisymmetric rigid shapes at constant speeds", Applied Ocean Research, Vol. 37, pp 183–197.
- Amin, W., Davis, M., Thomas, G. Holloway, D., 2012, "Analysis of Wave Induced Hull Vibrations using Continuous Wavelet Transforms", Ocean Engineering, Vol. 58, pp 154–166.
- Bardazzi, A., Lugni, C., Faltinsen, O.M., Graziani, G., 2012, "Hydroelastic study of the impact phenomena in sloshing flow", Hydroelasticity in marine technology, Tokyo, Japan.
- Begovic, E., Day, A.H., Incecik, A., 2011, "Experimental Ship Motion and Load Measurements in Head and Beam Seas", Proceedings of the 9th HSMV Symposium, Naples, Italy.
- Belenky, V. and Weems, K.M., 2012, "Dependence of roll and roll rate in nonlinear ship motions in following and stern quartering seas", Proceedings of the 11th International Conference on the Stability of Ships and Ocean Vehicles, Athens, Greece.



- Bellezi, C.A., Cheng, L.-Y., Nishimoto, K., 2013, "A Numerical Study of the Effects of Bow Shape on Green Water Phenomenon", 23rd ISOPE, Alaska, USA.
- Bennett, S.S., Hudson, D.A., Temarel, P., Price, W.G., 2012, "The influence of abnormal waves on global wave-induced loads", Hydroelasticity in marine technology, Tokyo, Japan.
- Besten, J.H. den, Huijsmans, R.H.M., Vredveldt, A., 2011, "Hydrodynamic impact of sandwich structures with vibration isolation and structural damping properties", International Shipbuilding Progress, Vol. 58(1), pp 1-57.
- Blendermann, W., 1994, "Parameter identification of wind loads on ships", Journal of Wind Engineering and Industrial Aerodynamics, Vol. 51, pp 339-351.
- Bogaert, H., Brosset, L., Kaminski, M.L., 2010, "Interaction between wave impacts and corrugations of MarkIII Containment System for LNG carriers: findings from the Sloshel project", 20th ISOPE, Beijing, China.
- Boom, H. van den, Hout, I. van der, Flikema, M., 2008, "Speed-Power Performance of Ships during Trials and in Service", SNAME Greek Section 2nd International Symposium on Ship Operations, Management & Economics, Athens, Greece, pp 1-7.
- Bouscasse, B., Broglia, R., Stern, F., 2013, "Experimental investigation of a fast catamaran in head waves", Ocean Engineering, Vol. 72, pp 318-330.
- Buchner, B. and van den Berg, J., 2013, "Non-linear Wave Reflection along the Side of Ships leading to Green Water on Deck", PRADS 2013, Changwon, Korea.
- Bunnik, T., Daalen, E. van, Kapsenberg, G., Shin, Y., Huijsmans, R., Deng, G., Delhommeau, G., Kashiwagi, M., Beck, B., 2010, "A comparative study on state-of-the-art prediction tools for seakeeping", 28th Symposium on Naval Hydrodynamics, California, USA, pp 1-13.
- Bureau Veritas, 2011, "New Guidance Note NI 554 Design Sloshing Loads for LNG Membrane Tanks", Bureau Veritas (BV), Classification Notes.
- Carrica, P.M., Wilson, R.V., Noack, R., Stern, F., 2007, "Ship motions using single-phase level set with dynamic overset grids", Computer & Fluids, Vol. 36, pp 1095-1111.
- Chen, Z.Y., Ren, H.-L., Li, H., Zhang, K.-H., 2012, "Experimental and numerical analysis of bow slamming and whipping in different sea states", Journal of Ship Mechanics, Vol. 16(3), pp 246-253.
- Chiu, F.C., Tiao, W.C., Guo, J., 2007, "Experimental study on the nonlinear pressure acting on a high-speed vessel in regular waves", Journal of Marine Science and Technology, Vol. 12, pp 230-217.
- Choi, H.I., Choi, Y.M., Kim, H.Y., Kwon, S.H., Park, J.S., Lee, K.H., 2010, "A study on the characteristic of piezoelectric sensor in sloshing experiment", 20th ISOPE, Beijing China.
- Chuang, Z.J. and Steen, S., 2013, "Speed loss of a vessel sailing in oblique waves", Ocean Engineering, Vol. 64, pp 88-99.



- Clauss, G.F. and Klein, M., 2011, "The New Year Wave in a seakeeping basin: Generation, propagation, kinematics and dynamics", Ocean Engineering, Vol. 38, pp 1624-1639.
- Colicchio, G., Colagrossi, A., Lugni, C., Brocchini, M., Faltinsen, O.M., 2007, "Challenges in the numerical investigation of the flip-through", 9th International Conference in Numerical Ship Hydrodynamics, Michigan, USA.
- Das, S. and Cheung, K.F., 2011, "Hydroelasticity of Marine Vessels Advancing in a Seaway", Proceedings of the 11th International Conference on Fast Sea Transportation, Hawaii, USA, pp. 192-200.
- Datta, R., Fonseca, N., Guedes Soares, C., 2013, "Analysis of the forward speed effects on the radiation forces on a Fast Ferry", Ocean Engineering, Vol. 60, pp 136-148.
- Det Norske Veritas (DNV), 2006, "Sloshing analysis of LNG membrane tanks", Det Norske Veritas (DNV), Classification Notes.
- Det Norske Veritas (DNV), 2010, "Environmental conditions and environmental loads", Recommended Practice DNV-RP-C205.
- Dommermuth, D.G., O'Shea, T.T., Wyatt, D.C., Ratcliffe, T., Weymouth, G.D., Hendrikson, K.L., Yue, D.K.P., Sussman, M., Adams, P., Valenciano, M., 2007, "An Application of Cartesian-Grid and Volume-of-Fluid Methods to Numerical Ship Hydrodynamics", 9th International Conference in Numerical Ship Hydrodynamics, Michigan, USA.
- Doring, M., Oger, G., Alessandrini, B., Ferrant, P., 2004, "SPH Simulations of Floating Bodies in Waves", 19th IWWF, Cortona, Italy.
- Du, S.X., Hudson, D., Price, W.G., Temarel, P., 2012, "An investigation into the hydrodynamic analysis of vessels with a zero or forward speed", Journal of Engineering for the Maritime Environment, Vol. 226(2), pp 83-102.
- Faltinsen, O.M., Minsaas, K.J., Liapis, N., Skjördal, S.O., 1980, "Prediction of resistance and propulsion of a ship in a seaway", 13th Symposium on Naval Hydrodynamics, Tokyo, Japan, pp 505-529.
- Faltinsen, O.M. and Sun, H., 2011, "Dynamic motions of planing vessels in head seas", Journal of Marine Science and Technology, Vol. 16, pp 168-180.
- Fonseca, N., Ricardo, P., Guedes, S.C., Clauss, G., Schmittner, C., 2010, "Numerical and experimental analysis of extreme wave induced vertical bending moments on a FPSO", Applied Ocean Research, Vol. 32, pp 374-390.
- French, B., Thomas, G., Davis, M., 2013, "Slam Occurrences and Loads of a High-Speed Wave Piercer Catamaran in Irregular Seas", Proceedings of the Institution of Mechanical Engineers, Part M: Journal of Engineering for the Maritime Environment, August, 2013.
- French, B., Thomas, G., Davis, M.R., 2014, "Slam Characteristics of a High-Speed Wave Piercing Catamaran in Irregular Waves", International Journal of Maritime Engineering, Vol. 156 (1), pp A-25 - A-36.



- Fujii, H. and Takahashi, T., 1975, "Experimental study on the resistance increase of a ship in regular oblique waves", Proceedings of the 14th ITTC, Ottawa, Canada, pp 351-360.
- Fujiwara, T. and Ueno, M., 2006, "Cruising performance of a large passenger ship in heavy sea", 16th ISOPE, San Francisco, USA.
- Gavory, T., 2005, "Innovative tools open up new prospects for liquid motion model tests", Proceedings of the Gastech, Bilbao, Spain.
- Graczyk, M., Moan, T., Rognebakke, O., 2006, "Probabilistic Analysis of Characteristic Pressure for LNG Tanks", Journal of Offshore Mechanics and Arctic Engineering, Vol. 128, pp 133-144.
- Gran, S., 1981, "Statistical distributions of local impact pressures in liquid sloshing", Norwegian Maritime Research, Vol. 9(2), pp 2-12.
- Greco, M., Bouscasse, B., Lugni, C., 2012, "3-D seakeeping analysis with water on deck and slamming. Part 2: Experiments and physical investigation", Journal of Fluids and Structures, Vol. 33, pp 148-179.
- Grin, R., 2012, "On the Prediction of Wave Added Resistance with Empirical Methods", Proceedings of 11th IMDC Conference, Glasgow, UK, pp 313-324.
- Guo, B.J. and Steen, S., 2010, "Experiment on added resistance in short waves", 28th Symposium on Naval Hydrodynamics, Pasadena, California.
- Guo, B.J. and Steen, S., 2011, "Evaluation of added resistance of KVLCC2 in short waves", Journal of Hydrodynamics, Vol. 23(6), pp 709-722.
- Guo, B.J., Steen, S., Deng, G.B., 2012, "Seakeeping prediction of KVLCC2 in head waves with RANS", Applied Ocean Research, Vol. 35, pp 56-67.
- Guo, L.-D., Sun, D.-P., Wu, H., 2012a, "A new numerical wave flume combining the 0-1 type BEM and the VOF method", Journal of Hydrodynamics, Vol. 24(4), pp 506-517.
- Halswell, P.K., Wilson, P.A., Taunton, D.J., Austen, S., 2011, "Design and performance of inflatable boats: Flexibility and environmental considerations", Proceedings of the 9th HSMV Symposium, Naples, Italy.
- Hashimoto, H., Umeda, N., Matsuda, A., 2011, "Broaching prediction of a wave-piercing tumblehome vessel with twin screws and twin rudders", Journal of Marine Science and Technology, Vol. 16, pp 448-461.
- He, G. and Kashiwagi, M., 2012, "Numerical analysis of the hydroelastic behavior of a vertical plate due to solitary waves", Journal of Marine Science and Technology, Vol. 17, pp 154-167.
- He, G. and Kashiwagi, M., 2013, "Higher-Order BEM for Radiation Forces of a Modified Wigley Hull with Forward Speed", 23rd ISOPE, Anchorage, Alaska.
- Hong, S.Y. and Nam, B.-W., 2011, "Analysis of 2nd-Order Wave Force on Floating Bodies Using FEM in Time Domain", International Journal of Offshore and Polar Engineering, Vol. 21(1), pp 22-28.



- Hu, C. and Kashiwagi, M., 2007, "Numerical and Experimental Studies on Three-Dimensional Water on Deck with a Modified Wigley Model", 9th International Conference in Numerical Ship Hydrodynamics, Michigan, USA.
- Hu, C., Kashiwagi, M., Sueyoshi, M., 2008, "Improvement towards High-Resolution Computation on Strongly Nonlinear Wave-Induced Motions of an Actual Ship", 27th Symposium on Naval Hydrodynamics, Seoul, Korea.
- Hughes, M.J. and Weems, K.M., 2011, "Time-Domain Seakeeping Simulations for a High Speed Catamaran with an Active Ride Control System", Proceedings of the 11th International Conference on Fast Sea Transportation, Hawaii, USA.
- Ichinose, Y., Tsujimoto, M., Shiraishi, K., Sogihara, N., 2011, "Decrease of Ship Speed in Actual Seas of a Bulk Carrier in Full Load and Ballast Conditions", Journal of the Japan Society of Naval Architects and Ocean Engineers, Vol. 15, pp 37-45.
- Iijima, K., Itamura, N., Fujikubo, M., 2011, "Comparison of Long-term Fatigue Damage in Bulk Carrier, VLCC and Container Carrier Subjected to Wave-induced Vibrations", Proceedings of the 11th International Conference on Fast Sea Transportation, Hawaii, USA, pp. 547-554.
- IMO MEPC.1/Circ.796 12, 2012, "Interim Guidelines for the Calculation of the Coefficient f_w for Decrease in Ship Speed in a Representative Sea Condition for Trial Use".
- IMO MEPC64/4/15 29, 2012a, "ITTC Recommended Procedure 7.5-04-01-01.2, "Speed/power trials, part 2, analysis of speed/power trial data"".
- IMO MEPC64/INF.6 29, 2012b, "Additional information on ITTC Recommended Procedure 7.5-04-01-01.2, "Speed/power trials, part 2, analysis of speed/power trial data"".
- Jacobi, G., Thomas, G., Davis, M.R., Davidson, G., 2014, "An insight into the slamming behaviour of large high-speed catamarans through full-scale measurements" Journal of Marine Science and Technology, Vol. 19(1), pp 15-32.
- Ji, Y.M., Shin, Y.S., Park, J.S., Hyun, J.M., 2012, "Experiments on non-resonant sloshing in a rectangular tank with large amplitude lateral oscillation", Ocean Engineering, Vol. 50, pp 10-22.
- Joncquez, S.A.G., 2009, "Second-Order Forces and Moments Acting on Ships in Waves," PhD Thesis, Technical University of Denmark, Copenhagen, Denmark.
- Kashiwagi, M. and Ohkusu, M., 1993, "Study on the Wave-Induced Steady Force and Moment", Journal of The Society of Naval Architects of Japan, Vol. 173, pp 185-194.
- Kim, B., Ryu, M.C., Jung, J.H., Shin, Y.S., 2010, "Identification of critical sea states for sloshing model tests", Proceedings of the Society of Naval Architects & Marine Engineers, Washington, USA.
- Kim, H.I., Kwon, S.H., Park, J.S., Lee, K.H., Jeon, S.S., Jung, J.H., Ryu, M.C., Hwang, Y.S., 2009, "An Experimental Investigation of Hydrodynamic Impact on 2-D LNGC Models", 19th ISOPE, Osaka, Japan.



- Kim, J.-H., Kim, K.-H., Lee, D.-Y., Jung, B.-H., Kim, Y., 2013, "A Fully Coupled BEM-FEM Analysis on Ship Structural Hydroelasticity and Experimental Validation", PRADS 2013, Changwon, Korea, pp. 603-611.
- Kim, J.-H., Kim, Y., Kim, Y., Kim, K.-H., 2013a, "Study on Ship Structural Hydroelasticity and Fatigue Assessment in Irregular Seaways", OMAE 2013, Nantes, France.
- Kim, J.W., Tan, J.H.C., Magee, A., Wu, G., Paulson, S., Davies, B., 2013b, "Analysis of ringing response of a gravity based structure in extreme sea states", ASME 2013, Nantes, France.
- Kim, K.-H., Bang, J.-S., Kim, J.-H., 2013c, "Fully coupled BEM-FEM analysis for ship hydroelasticity in waves", Journal of Marine Structures, Vol. 33, pp 71-99.
- Kim, K.H. and Kim, Y., 2011, "Numerical study on added resistance of ships by using a time-domain Rankine panel method", Ocean Engineering, Vol. 38, pp 1357-1367.
- Kim, S., Kim, C.-Y., Cronin, D., 2013d, "Green Water Impact Loads on Breakwaters of Large Container Carriers", PRADS 2013, Changwon, Korea.
- Kim, S.Y., Kim, K.H., Kim, Y., 2012, "Comparative Study on Model-Scale Sloshing Tests", Journal of Marine Science and Technology, Vol. 17(1) pp 47-58.
- Kim, S. and Sung, Y.J. 2012, "Numerical simulations of maneuvering and dynamic stability of a containership in waves", Proceedings of the 11th International Conference on the Stability of Ships and Ocean Vehicles, Athens, Greece.
- Kim, T. and Kim, Y., 2011a, "Numerical analysis on floating-body motion responses in arbitrary bathymetry", Ocean Engineering, Vol. 62, pp 123-139.
- Kim, Y., 2007, "Experimental and numerical analyses of sloshing flows", Journal of Engineering Mathematics, Vol. 58, pp 191-210.
- Kim, Y., Kim, S.Y., Yoo, W.J., 2010a, "Statistical Evaluation of Local Impact Pressures in Sloshing". 20th ISOPE, Beijing, China.
- Kim, Y., Kim, S.Y., Kim, K.H., Chun, S.E., Suh, Y.S., Park, J.J., Hwang-Bo, S.M., Lee, Y.J., 2011, "Model-Scale Sloshing Tests for an Anti-Sloshing Floating Blanket System", 21st ISOPE, Hawaii, USA.
- Kim, Y., Kim, Y., Liu, Y., Yue, D.K.P., 2007, "On the Water-Entry Impact Problem of Asymmetric Bodies", 9th International Conference in Numerical Ship Hydrodynamics, Michigan, USA.
- Kishev, Z.R., Hu, C., Kashiwagi, M., 2006, "Numerical simulation of violent sloshing by a CIP-based method", Journal of Marine Science and Technology, Vol. 11 pp 111-122.
- Kitagawa, Y., Tanizawa, K., Tsukada, Y., 2014, "Development of an Experimental Methodology for Self-Propulsion Test with a Marine Diesel Engine Simulator, Third Report – Auxiliary Thruster System -", Proceedings of the 24th ISOPE conference, Vol.3, pp 691-696.



- Kjellberg, M., Contento, G., Janson, C.E., 2011, "A Nested Domains Technique for a Fully-Nonlinear Unsteady Three-Dimensional Boundary Element Method for Free-Surface Flows with Forward Speed", 21st ISOPE, Hawaii, USA.
- Koning, J. and Kapsenberg, G., 2012, "Full scale container ship cross section loads - First results", Hydroelasticity in marine technology, Tokyo, Japan.
- Korobkin, A.A., 2011, "Semi-analytical approach in Generalized Wagner Model", 26th IWWF, Athens, Greece.
- Korobkin, A.A., 2013, "Wagner-type models of water impact with separation for a finite wedge", 28th IWWF, Marseille, France.
- Kuo, J.F., Campbell, R.B., Ding, Z., Hoie, S.M., Rinehart, A.J., Sandström, R.E., Yung, T.W., Greer, M.N., Danaczko, M.A., 2009, "LNG Tank Sloshing Assessment Methodology – The New Generation", 19th ISOPE, Osaka, Japan.
- Kuroda, M., Tsujimoto, M., Fujiwara, T., Ohmatsu, S., Takagi, K., 2008, "Investigation on Components of Added Resistance in Short Waves", Journal of the Japan Society of Naval Architects and Ocean Engineers, Vol. 8, pp 141-146.
- Kuroda, M., Tsujimoto, M., Sogihara, N., 2012, "Onboard Measurement for a Container Ship in view of Container Load Condition", Journal of the Japan Society of Naval Architects and Ocean Engineers, Vol. 15, pp 29-35.
- Larsson, L., Stern, F., Visonneau, M., 2010, "Gothenburg 2010: A Workshop on Numerical Ship Hydrodynamics", Gothenburg, Sweden.
- Larsson, L., Stern, F., Visonneau, M., 2011, "CFD in Ship Hydrodynamics – Results of the Gothenburg 2010 Workshop", MARINE 2011 – IV International Conference on Computational Methods in Marine Engineering, Lisbon, Portugal.
- Larsson, L., Stern, F., Visonneau, M., 2014, "Numerical Ship Hydrodynamics – an assessment of the Gothenburg 2010 Workshop", Springer.
- Lavroff, J., Davis, M., Holloway, D., Thomas, G., 2013, "Wave Slamming Loads on Wave-Piercer Catamarans Operating at High-Speed Determined by Hydroelastic Segmented Model Experiments", Marine Structures, Vol. 33, pp. 120-142.
- Lloyd's Register (LR), 2009, "Sloshing Assessment Guidance Document for Membrane Tank LNG Operations", Lloyd's Register (LR), Classification Notes.
- Loysel, T., Chollet, S., Gervaise, E., Brosset, L., De Seze, P.-E., 2012, "Results of the First Sloshing Model Test Benchmark", 22nd ISOPE, Rhodes, Greece.
- Maillard, S. and Brosset, L., 2009, "Influence of Density Ratio between Liquid and Gas on Sloshing Model Test Results", 19th ISOPE, Osaka, Japan.
- Maruo, H., 1960, "The drift of a body floating on waves," Journal of Ship Research, Vol. 4, pp 1-10.
- Mathiesen, J., 1976, "Sloshing loads due to random pitching", Norwegian Maritime Research, Vol. 4(3), pp 2-13.



- Matsubara, S., Thomas, G., Davis, M.R., Holloway, D.S., Roberts, T., 2011, "Influence of Centrebow on Motions and Loads of High-Speed Catamarans", Proceedings of the 11th International Conference on Fast Sea Transportation, Hawaii, USA, pp 661-668.
- Maximo, R., Ruggeri, F., Mueller, C., 2012, "Parametric Design Tool Considering Integrated Seakeeping, Stability and Wave Resistance of a High Speed Trimaran Vessel", Proceedings of the 8th International Conference on High-Performance Marine Vehicles (HIPER), Mülheim an der Ruhr, Germany.
- Moctar, B., Kaufmann, J., Ley, J., Oberhagemann, J., Shigunov, V., Zorn, T., 2010, "Prediction of ship resistance and ship motions using RANSE", Göteborg 2010: A workshop on CFD in Ship Hydrodynamics, Göteborg, Sweden, pp 495-505.
- Monroy, C., Ducrozet, G., Roux de Reilhac, P., Gentaz, L., Ferrant, P., Alessandrini, B., 2009, "RANS Simulations of Ship Motions in Regular and Irregular Head Seas using the SWENSE Method", 19th ISOPE, Osaka, Japan.
- Mortola, G., Incecik, A., Turan, O., Hirdaris, S., 2011, "Large Amplitude Motions and Loads Using a Non-linear 2D Approach", 26th IWWFEB, Athens, Greece.
- Nam, B.W. and Kim, Y., 2006, "Simulation of Two-Dimensional Sloshing Flows by SPH Method", 16th ISOPE, San Francisco, California, USA.
- Nan, X. and Vassalos, D., 2012, "A three dimensional numerical study for ship motion in waves with forward speed", Proceedings of the 11th International Marine Design Conference, Glasgow, UK.
- Nippon Kaiji Kyokai (NK), 2010, "Guideline for the Technical Appraisal of Ship Performance in Actual Seas", Nippon Kaiji Kyokai (NK), Classification Notes, pp 1-27.
- Nitin, R., Tam, T., Krish, T., Dominique, R., Robert, K.M., Timothy, F., 2010, "The Effect of Sampling Rate on the Statistics of Impact Pressure", OMAE 2010, Shanghai, China.
- Ogawa, Y., Kitamura, O., Toyoda, M., 2012, "A study for the statistical characteristic of slamming induced vibration of large container ship", Hydroelasticity in Marine Technology, Tokyo, Japan.
- Oger, G., Brosset, L., Guilcher, P.-M., Jacquin, E., Deuff, J.-B., Le Touzé, D., 2009, "Simulations of Hydro-elastic Impacts Using a Parallel SPH Model", 19th ISOPE, Osaka, Japan.
- Oger, G., Doring, M., Alessandrini, B., Ferrant, P., 2006, "Two-dimensional SPH Simulations of Wedge Water Entries", Journal of Computational Physics, Vol. 213, pp 803-822.
- Oger, G., Rousset, J.M., Le Touzé, D., Alessandrini, B., Ferrant, P., 2007, "SPH simulations of 3-D slamming problems", 9th International Conference in Numerical Ship Hydrodynamics, Michigan, USA.



- Ommani, B. and Faltinsen, O.M., 2011, "Study on Linear 3D Rankine Panel Method for Prediction of Semi-Displacement Vessels' Hydrodynamic Characteristics at High Speed", Proceedings of the 11th International Conference on Fast Sea Transportation, Hawaii, USA.
- Orihara, H. and Miyata, H., 2003, "Evaluation of added resistance in regular incident waves by computational fluid dynamics motion simulation using an overlapping grid system", Journal of Marine Science and Technology, Vol. 8, pp 47-60.
- Panciroli, R., 2012, "Water entry of flexible wedges: Some issues on the FSI phenomena", Applied Ocean Research Vol. 39, pp 72-74.
- Paredes, R., Imas., L., 2011, "Application of SPH in Fluid-Structure Interaction Problems Involving Free-surface Hydrodynamics", Proceedings of the 11th International Conference on Fast Sea Transportation, Hawaii, USA, pp 200-208.
- Pastoor, W., Tveitnes, T., Valsgård, S., Sele, H.O., 2004, "Sloshing in Partially filled LNG Tanks – an Experimental Survey", Offshore Technology Conference, Houston, Texas, USA.
- Peric, M. and Schreck, E., 2012, "Simulation of extreme motion of floating bodies using overlapping grids", NuTTS2012: 15th Numerical Towing Tank Symposium, Cortona, Italy.
- Piro, D.J. and Maki, K.J., 2011, "Hydroelastic Wedge Entry and Exit", Proceedings of the 11th International Conference on Fast Sea Transportation, Hawaii, USA, pp 653-660.
- Pistani, F., and Thiagarajan, K., 2010, "Set-up of a Sloshing Laboratory at the University of Western Australia", 20th ISOPE, Beijing, China.
- Rahaman, M. and Akimoto, H., 2012, "Analysis of the Mechanism of Slamming on the Bow Flare Region of a Container Ship Using RaNS CFD Method", 22nd ISOPE, Rhodes, Greece.
- Rijkens, A.A.K., 2013, "Improving the sea keeping behaviour of fast ships using a proactive ride control system", Proceedings of the 12th International Conference on Fast Sea Transportation, Amsterdam, Netherlands.
- Rijkens, A.A.K., Keuning, J.A., Huijsmans, R.H.M., 2011, "A computational tool for the design of ride control systems for fast planing vessels" International Shipbuilding Progress, Vol. 58, pp 165-190.
- Riley, M.R., Coats, T., Haupt, K., Jacobson, D., 2011, "Ride Severity Index – A New Approach to Quantifying the Comparison of Acceleration Responses of High-Speed Craft", Proceedings of the 11th International Conference on Fast Sea Transportation, Hawaii, USA.
- Rose, C.J., Weil, C.R., Troesch, A.W., 2011, "Planing Craft Acceleration Prediction Using Vibro-Impact Methodology", Proceedings of the 11th International Conference on Fast Sea Transportation, Hawaii, USA.
- Ryu, M.C., Jung, J.H., Jeon, S.S., Hwang, Y.S., Han, S.K., Kim, Y.S., Cho, T.I., Kwon, S.H., 2009, "Reference Load for a Conventional 138K CBM LNG Carrier in a Comparative Approach", OMAE 2009, Honolulu, Hawaii, USA.



- Sadat-Hosseini, H., Wu, P., Carrica, P.M., Kim, H., Toda, Y., Stern, F., 2013, "CFD verification and validation of added resistance and motions of KVLCC2 with fixed and free surge in short and long head waves", Ocean Engineering, Vol. 59, pp 240-273.
- Salvesen, N., Tuck, E.O., Faltinsen, O.M., 1970, "Ship Motions and Sea Loads," Transactions of Society of Naval Architects and Marine Engineers, Vol. 78, pp 250-279.
- Senjanović, I., Hadžić, N., Bigot, F., 2013, "Finite element formulation of different restoring stiffness issues in the ship hydroelastic analysis and their influence on response", Ocean Engineering, Vol. 59, pp 198-213.
- Senjanović, I., Hadžić, N., Tomić, M., 2011, "Investigation of Restoring Stiffness in the Hydroelastic Analysis of Slender Marine Structures", Journal of Offshore Mechanics and Arctic Engineering, Vol. 133(3).
- Seo, M.G., Lee, J.H., Yang, K.K., Kim, K.H., Kim, Y., 2013, "Analysis of added resistance: comparative study on different methodologies", OMAE 2013, Nantes, France.
- Seo, M.G., Park, D.M., Kim, K.H., Kim, Y., 2012, "Computation on Added Resistance Based on Near-Field and Far-Field Methods", 22nd ISOPE, Rhodes, Greece.
- Shao, Y-L. and Faltinsen, O.M., 2012, "A numerical study of the second-order wave excitation of ship springing in infinite water depth", Journal of Engineering for the Maritime Environment, Vol. 226(2), pp 103-119.
- Simonsen, C.D., Otzen, J.F., Joncquez, S., Stern, F., 2014, "EFD and CFD for KCS heaving and pitching in regular head waves", Journal of Marine Science and Technology, Vol. 18, pp 435-459.
- Skejic, R. and Faltinsen, O.M., 2013, "Maneuvering Behavior of Ships in Irregular Waves", OMAE 2013, Nantes, France.
- Soding, H., Shigunov, V., Schellin, T.E., el Moctar, O., Walter, S., 2012, "Computing added resistance in waves – Rankine panel method vs RANSE method", NuTTS2012: 15th Numerical Towing Tank Symposium, Cortona, Italy.
- Sogihara, N., Ueno, M., Fujiwara, T., Tsujimoto, M., Sasaki, N., 2011, "Onboard Measurement for Verification of a Calculation Method on Decrease of Ship Speed for a RoRo Cargo Ship and an Oil Tanker", 21st ISOPE, Hawaii, USA.
- Sogihara, N., Ueno, M., Hoshino, K., Tsujimoto, M., Sasaki, N., 2010, "Verification of Calculation Method on Ship Performance by Onboard Measurement", 20th ISOPE, Beijing, China.
- Song, M-J., Kim, K.-H., Kim, Y., 2011, "Numerical analysis and validation of weakly nonlinear ship motions and structural loads on a modern containership", Ocean Engineering, Vol. 38(1), pp 77-87.
- Specialist Committee on Performance of Ships in Service 27th ITTC, 2012, "Speed and Power Trials Analysis of Speed/Power Trial Data", ITTC – Recommended Procedures and Guidelines.



- Stenius, I., Rosén, A., Battley, M., Allen, T., Pehrson, P., 2011, "Hydroelastic Effects in Slamming Loaded Panels". Proceedings of the 11th International Conference on Fast Sea Transportation, Hawaii, USA, pp. 644-652.
- Sueyoshi, M., 2004, "Numerical Simulation of Extreme Motions of a Floating Body by MPS Method", Proceedings of the Joint International Conference of OCEANS'04 and TECHNO-OCEAN, Kobe, Japan.
- Sueyoshi, M., Kishev, Z.R., Kashiwagi, M., 2005, "A Particle Method for Impulsive Loads Caused by Violent Sloshing", 20th IWWFEB, Spitsbergen, Norway.
- Swidan, A., Amin, W., Ranmuthugala, D., Thomas, G., Penesis, I., 2013, "Numerical prediction of symmetric water impact loads on wedge shaped hull form using CFD", World Journal of Mechanics, Vol. 3(8).
- Tanizawa, K., Kitagawa, Y., Takimoto, T., Tsukada, Y., 2012, "Development of an Experimental Methodology for Self-Propulsion Test With a Marine Diesel Engine Simulator", International Journal of Offshore and Polar Engineering, Vol.23, No.3, pp. 197-204
- Tello, M., Ribeiro e Silva, S., Guedes Soares, C., 2011, "Seakeeping performance of fishing vessels in irregular waves", Ocean Engineering, Vol. 38(5-6), pp 763-773.
- Thomas, G., Matsubara, S., Davis, M.R., French, B., Lavroff, J., Amin, W., 2012, "Lessons learnt through the design, construction and testing of a hydroelastic model for determining motions, loads and slamming behaviour in severe sea states", Hydroelasticity in marine technology, Tokyo, Japan.
- Thomas, G., Winkler, S., Davis, M.R., Holloway, D., Matsubara, S., Lavroff, J., French, B., 2011, "Slam events of high-speed catamarans in irregular waves", Journal of Marine Science and Technology, Vol. 16, pp 8-21.
- Tiao, W.C., 2011, "Experimental investigation of nonlinearities of ship responses in head waves", Applied Ocean Research, Vol. 33, pp 60-68.
- Tong, X.-W., Li, H., Ren, H.-L., 2013, "A hybrid approach applied to fast calculating the time-domain ship motions", Journal of Ship Mechanics, Vol. 17(7), pp 756-762.
- Tsujimoto, M., Kuroda, M., Shibata, K., Sogihara, N., Takagi, K., 2009, "On a Calculation of Decrease of Ship Speed in Actual Seas", Journal of the Japan Society of Naval Architects and Ocean Engineers, Vol. 9, pp 79-85.
- Tsujimoto, M., Kuroda, M., Shiraishi, K., Ichinose, Y., Sogihara, N., 2012, "Verification on the Resistance Test in Waves Using the Actual Sea Model Basin", Journal of the Japan Society of Naval Architects and Ocean Engineers, Vol. 16, pp 33-39.
- Tsujimoto, M., Sasaki, N., Takagi, K., 2011, "On the Evaluation Method of Ship Performance for Blunt Ships", Journal of the Japan Society of Naval Architects and Ocean Engineers, Vol. 15, pp 21-27.



- Tsujimoto, M., Sasaki, N., Takagi, K., 2012a, "On the Evaluation Method of Ship Performance for Blunt Ships - Extension of 10 mode Index for Ships", Journal of the Japan Society of Naval Architects and Ocean Engineers, Vol. 15, pp 21-27.
- Tsujimoto, M., Shibata, K., Kuroda, M., Takagi, K., 2008, "A Practical Correction Method for Added Resistance in Waves", Journal of the Japan Society of Naval Architects and Ocean Engineers, Vol. 8, pp 147-154.
- Visonneau, M., Queutey, P., Leroyer, A., Deng, G.B., Guilmineau, E., 2008, "Ship Motions in Moderate and Steep Waves with an Interface Capturing Method", 8th ICHD, Nantes, France, pp.485-492.
- Walree, F. van, 2012, "Development and validation of a time domain seakeeping code for a destroyer hull form operating in extreme sea states", Proceedings of the 11th International Conference on the Stability of Ships and Ocean Vehicles, Athens, Greece.
- Walree, F. van and de Jong, P., 2011, "Validation of a Time Domain Panel Code for High Speed Craft operating in Stern Quartering Seas", Proceedings of the 11th International Conference on Fast Sea Transportation, Hawaii, USA.
- Walree, F. van and Turner, T., 2013, "Development And Validation Of A Time Domain Panel Code For Prediction Of Hydrodynamic Loads On High Speed Craft", Proceedings of the 12th International Conference on Fast Sea Transportation, Amsterdam, Netherlands.
- Wang, J. and Xie, B., 2012, "A simplified method for predicting global motion of moored semi-submersible platforms", 22nd ISOPE, Rhodes, Greece.
- Wang, X.L., Gu, X.K., Hu, J.J., Xu, C., 2012, "Investigation of sloshing and its effects on global responses of a large LNG carrier by experimental method", Journal of Ship Mechanics, Vol. 16(12), pp 1394-1401.
- Wemmenhove, R., Iwanowski, B., Lefranc, M., Veldman, A.E.P., Luppens, R., Bunnik, T., 2009, "Simulation of Sloshing Dynamics in a Tank by an Improved Volume-of-Fluid Method", 19th ISOPE, Osaka, Japan.
- Weymouth, G.D. and Yue, D.K.P., 2013, "Physics-Based Learning Models for Ship Hydrodynamics", Journal of Ship Research, Vol. 57(1), pp 1-12.
- White, N., Wang, Z., Lee, Y., 2012, "Guidance Notes on Whipping and Springing Assessment", Proceedings of the 11th International Marine Design Conference (IMDC 2012), Glasgow, UK.
- Wu, M.K., Lehn, E., Moan, T., 2012, "Design of segmented model for ship seakeeping tests with hydroelastic effects", Hydroelasticity in marine technology, Tokyo, Japan.
- Wu, M.K. and Stambaugh, K., 2013, "Experimental And Numerical Study Of Hydroelastic Responses In A High-Speed Vessel", Proceedings of the 12th International Conference on Fast Sea Transportation, Amsterdam, Netherlands.
- Xie, N. and Vassalos, D., 2012, "Evaluation of the m-terms and 3D ship motions in waves", Journal of Ship Mechanics, Vol. 16(9), pp 971-979.



- Xu, G., Duan, W.-Y., 2013, "Time-domain simulation of wave-structure interaction based on multi-transmitting formula coupled with damping zone method for radiation boundary condition", Applied Ocean Research, Vol. 42, pp 136-143.
- Yamada, Y., Takami, T., Oka, M., 2012, "Numerical Study on the Slamming Impact of Wedge Shaped Obstacles considering Fluid-Structure Interaction (FSI)", 22nd ISOPE, Rhodes, Greece.
- Yan, S. and Ma, Q.W., 2011, "Fully Nonlinear Hydrodynamic Interaction Between Two 3D Floating Structures in Close Proximity", International Journal of Offshore and Polar Engineering, Vol. 21(3), pp 662-669.
- Yang, J., Kim, S., Park, J.S., Jung, B-H., Lee T-L., 2013, "Numerical Analysis for Slamming Impact Loads and Dynamic Structural Responses of a Containership" PRADS 2013, Changwon, Korea.
- Yang, K.K., Nam, B.W., Lee, J.H., Kim, Y., 2013a, "Numerical Analysis of Large-Amplitude Ship Motions Using FV-based Cartesian Grid Method", International Journal of Offshore and Polar Engineering, Vol. 23(3), pp 186-196.
- You, J. and Faltinsen, O.M., 2012, "A 3D Fully Nonlinear Numerical Wave Tank with a Moored Floating Body in Shallow Water", 22nd ISOPE, Rhodes, Greece.
- Yu, L., Ma, N., Gu, X., 2012, "Ship dynamic stability in rough seas", Proceedings of the 11th International Conference on the Stability of Ships and Ocean Vehicles, Athens, Greece.
- Yung, T.W., Ding, Z., He, H., Sandström, R.E., 2009, "LNG Sloshing: Characteristics and Scaling Laws," International Journal of Offshore and Polar Engineering, Vol. 19(4), pp 264-270.
- Zaraphonitis, G., Grigoropoulos, G.J., Damala, D.P., Mourkoyannis, D., 2011, "Seakeeping Analysis of a Medium-Speed Twin-Hull Containership", Proceedings of the 11th International Conference on Fast Sea Transportation, Hawaii, USA.
- Zhang, S., Weems, K., Lin, W.-M., 2011, "Solving Nonlinear Wave-Body Interaction Problems with the Pre-Corrected Fast Fourier Transform (pFFT) Method", Proceedings of the 11th International Conference on Fast Sea Transportation, Hawaii, USA.
- Zhang, Y., Wang, X., Tang, Z., Wan, D., 2013, "Numerical Simulation of Green Water Incidents Based on Parallel MPS Method", 23rd ISOPE, Anchorage, Alaska, USA.
- Zhao, W.-H., Hu, Z.-Q., Yang, J.-M., Wei, Y.-F., 2011, "Investigation on sloshing effects of tank liquid on the FLNG vessel responses in frequency domain", Journal of Ship Mechanics Vol.15(3), pp 227-237.
- Zhao, X.Z. and Hu, C.H., 2012, "Numerical and experimental study on a 2-D floating body under extreme wave conditions", Applied Ocean Research, Vol. 35, pp 1-13.